Article

Current Biology

# Genomic and physiological changes in a sexually selected and frugivorous bird radiation

## Highlights

- Sensory system, muscle, and diet-related genes show signatures of selection
- Sweet sensing (through T1R1-T1R3) evolved at the base of the manakin radiation
- Reduced lactase-phlorizin hydrolase activity coincided with an early diet shift
- Shifts in breeding systems and plumage are linked with transitions to frugivory

## Authors

Christopher N. Balakrishnan, Yasuka Toda, Meng-Ching Ko, ..., Bette A. Loiselle, Michael J. Braun, Maude W. Baldwin

## Correspondence

christopher.balakrishnan@gmail.com (C.N.B.), toda.y.e867@m.isct.ac.jp (Y.T.), maude.baldwin@bi.mpg.de (M.W.B.)

## In brief

Balakrishnan et al. take an integrative approach to explore the evolution of manakins, a frugivorous bird lineage with elaborate courtship displays. They detect genome-wide signatures related to sexual selection and diet and identify functional changes in taste receptors and digestive enzymes likely related to an early shift toward intensified frugivory.

Balakrishnan et al., 2026, Current Biology *36*, 1–16
June 22, 2026 
https://doi.org/10.1016/j.cub.2026.05.021

CellPress

Please cite this article in press as: Balakrishnan et al., Genomic and physiological changes in a sexually selected and frugivorous bird radiation, Current Biology (2026), https://doi.org/10.1016/j.cub.2026.05.021

Current Biology

CellPress
OPEN ACCESS

Article

# Genomic and physiological changes in a sexually selected and frugivorous bird radiation

Christopher N. Balakrishnan,[1,2,3,58,*] Yasuka Toda,[4,5,58,*] Meng-Ching Ko,[6,58] Morgan E. Wirthlin,[7,8,9,58] Robert J. Driver,[1,10,58] Peri E. Bolton,[1,3,58] Eliot T. Miller,[11,12,58] Daniel Mendez-Aranda,[6,13,58] Rebecca B. Dikow,[14] Paul B. Frandsen,[15] Elsie H. Shogren,[16,17] Kevin F.P. Bennett,[3,18] H. Luke Anderson,[3,19] Madeline G. Bursell,[15,20] Julia F. Cramer,[6] Keren R. Sadanandan,[6,21] Tomoya Nakagita,[4] Marco A. Pizo,[22]

*(Author list continued on next page)*

[1]Department of Biology, East Carolina University, 101 E. 10th Street, Greenville, NC 27858, USA
[2]Division of Environmental Biology, National Science Foundation, 401 Dulany Street, Alexandria, VA 22314, USA
[3]Department of Vertebrate Zoology, National Museum of Natural History, Smithsonian Institution, 10th St. & Constitution Ave. NW, Washington, DC 20560, USA
[4]Department of Agricultural Chemistry, School of Agriculture, Meiji University, 1-1-1 Higashi-Mita, Tama-ku, Kawasaki, Kanagawa 214-8571, Japan
[5]School of Life Science and Technology, Institute of Science Tokyo, 4259 Nagatsuta-cho, Midori-ku, Yokohama, Kanagawa 226-8501, Japan
[6]Evolution of Sensory and Physiological Systems Department, Max Planck Institute for Biological Intelligence, Am Klopferspitz 18, 82152 Planegg, Germany
[7]Department of Computational Biology, School of Computer Science & Neuroscience Institute, Carnegie Mellon University, 5000 Forbes Avenue, Pittsburgh, PA 15213, USA
[8]Department of Behavioral Neuroscience, Oregon Health & Science University (OHSU), 3181 SW Sam Jackson Park Road, Portland, OR 97239, USA
[9]Allen Institute, 615 Westlake Avenue N, Seattle, WA 98109, USA
[10]Duke University, 2138 Campus Drive, Durham, NC 27708, USA
[11]Center for Avian Population Studies, Cornell Lab of Ornithology, 159 Sapsucker Woods Road, Ithaca, NY 14850, USA
[12]American Bird Conservancy, P.O. Box 249, The Plains, VA 20198, USA
[13]Molecular Physiology of Somatic Sensation Laboratory, Max Delbrück Center for Molecular Medicine in the Helmholtz Association (MDC), Robert-Rössle-Straße 10, 13125 Berlin, Germany

*(Affiliations continued on next page)*

## SUMMARY

Across diverse organisms, the strength and ecological drivers of sexual selection vary enormously. In birds, some of the families with the most elaborate plumage and display—such as birds of paradise, manakins, and cotingas—are also specialist frugivores, yet links between shifts in diet, changes in breeding system, and the evolution of elaborate traits are poorly understood. We focus on manakins, a radiation of frugivorous Neotropical birds well known for spectacular courtship rituals and colorful plumage, and present an integrative analysis of the transition in both diet and mating systems in this clade to examine the causes and consequences of strong sexual selection. In manakins, we find reduced genetic diversity on the Z sex chromosome relative to autosomes, a predicted signature of sexual selection. We also identify targets of positive selection across the manakin radiation, including genes related to muscle function, visual perception, and the transition to frugivory. Among these, we observe selection on sugar-sensing taste receptors, as well as on lactase-phlorizin hydrolase, implicated in the consumption of chemically defended fruits. For both, we confirm that selection signatures correspond to functional changes and infer the relative time of these changes, as well as of shifts in diet, breeding systems, and plumage coloration: elaborated traits evolved subsequent to changes in mating systems and after key physiological changes facilitating fruit-eating. Altogether, these results suggest that intensified frugivory set the stage for the radiation of one of the planet's most colorful and acrobatic avian lineages.

## INTRODUCTION

Remarkable morphological and behavioral diversity can evolve as a result of intense sexual selection and competition for mates.[1,2] The acrobatic energy-intensive courtship displays of manakins, a family of suboscine passerine birds known for colorful and elaborate male plumage (Figures 1A and 1B), are thought to be the product of intense sexual selection[3]: males

Please cite this article in press as: Balakrishnan et al., Genomic and physiological changes in a sexually selected and frugivorous bird radiation, Current Biology (2026), https://doi.org/10.1016/j.cub.2026.05.021



Daniel S. Caetano,[23] Marina Anciães,[24] Carolina F. Ferreira,[25] Jacob S. Berv,[26,27] Kira M. Long,[28,29] Haw Chuan Lim,[30] Andre E. Moncrieff,[31,32] Sarah E. Kingston,[33] Noor D. White Carreiro,[3,34] Samantha R. Friedrich,[8] Camilo Alfonso Cuta,[35] James B. Pease,[17,36] Alexander A. Nevue,[8] Chad Tomlinson,[37] Aleksey Zimin,[38] Matthew I.M. Louder,[1] Michael S. Brewer,[1] Rachael A. Bay,[39] Kristen Ruegg,[40] Thomas B. Smith,[41,42] Yoshiro Ishimaru,[4] Andreas R. Pfenning,[7] Carolina Frankl-Vilches,[43] Manfred Gahr,[43] Claudio V. Mello,[8] Rebecca T. Kimball,[44] Edward L. Braun,[44]

*(Author list continued on next page)*

[14]Yale Library, Yale University, 120 High Street, New Haven, CT 06511, USA
[15]Department of Plant and Wildlife Sciences and Bean Life Science Museum, Brigham Young University, 4105 LSB, Provo, UT 84602, USA
[16]Division of Biology, Kansas State University, 116 Ackert Hall, Manhattan, KS 66506, USA
[17]Department of Biology, Wake Forest University, 1834 Wake Forest Road, Winston-Salem, NC 27109, USA
[18]Department of Biology and Biological Sciences Graduate Program, University of Maryland, 4094 Campus Drive, College Park, MD 20742, USA
[19]Department of Ecology & Evolutionary Biology, Tulane University, 6823 St. Charles Avenue, New Orleans, LA 70118, USA
[20]Bioinformatics Research Center, North Carolina State University, 1 Lampe Drive, Raleigh, NC 27607, USA
[21]Department of Biological Sciences, National University of Singapore, 14 Science Drive 4, Singapore 117543, Singapore
[22]Center for Research on Biodiversity and Climate Change (CBioClima), Departament of Biodiversity, São Paulo State University (UNESP), Rio Claro, Av. 24-A, 1515, Bela Vista, Rio Claro, São Paulo 13506–900, Brazil
[23]Department of Biological Sciences, Towson University, 8000 York Road, Towson, MD 21252, USA
[24]Biodiversity Coordination, National Institute of Amazon Research (INPA), Av. André Araújo, 2936, Aleixo, Manaus, AM 69067-375, Brazil
[25]Graduate Program in Genetics, Conservation and Evolutionary Biology (GCBv), National Institute for Research in the Amazon (INPA), Av. André Araújo, 2936, Aleixo, Manaus 69067-375, Brazil
[26]Department of Ecology and Evolutionary Biology, University of Michigan, 1105 N University Avenue, Ann Arbor, MI 48109, USA
[27]Museum of Paleontology, University of Michigan, 1105 N University Avenue, Ann Arbor, MI 48109, USA
[28]Program in Ecology, Evolution, and Conservation Biology, University of Illinois Urbana-Champaign, 505 S. Goodwin Avenue, Urbana, IL 61801, USA
[29]Center for Conservation Genomics, Smithsonian National Zoo and Conservation Biology Institute, 3001 Connecticut Ave. NW, Washington, DC, 20008, USA
[30]Department of Biology, George Mason University, 4400 University Drive, VA, Fairfax 22030, USA
[31]Department of Biological Sciences and Museum of Natural Science, Louisiana State University, 119 Foster Hall, Baton Rouge, LA 70803, USA
[32]Center for Conservation Genomics, Smithsonian National Zoo and Conservation Biology Institute, 3001 Connecticut Ave. NW, Washington, DC, 20008, USA
[33]Sea Education Association, 171 Woods Hole Road, Woods Hole, MA 02543, USA
[34]Biological Imaging Core, National Eye Institute, National Institutes of Health, 6 Center Drive, Bethesda, MD 20892, USA
[35]Department of Biological Sciences, Virginia Tech, 926 West Campus Drive, Blacksburg, VA 24061, USA
[36]Department of Evolution, Ecology, and Organismal Biology, The Ohio State University, 318 W. 12th Avenue, Columbus, OH 43210, USA
[37]McDonnell Genome Institute, Washington University, 4444 Forest Park Avenue, St Louis, MO 63108, USA
[38]Department of Biomedical Engineering, Johns Hopkins University, 3400 N. Charles Street, Baltimore, MD 21218, USA
[39]Department of Evolution and Ecology, University of California, Davis, One Shields Avenue, Davis, CA 95616, USA
[40]Department of Biology, Colorado State University, 1878 Campus Delivery, Fort Collins, CO 80523, USA
[41]Department of Ecology and Evolutionary Biology, University of California, Los Angeles, 610 Charles E. Young Drive South, Los Angeles, CA 90095, USA
[42]Center for Tropical Research, Institute of the Environment and Sustainability, University of California, Los Angeles, 619 Charles E. Young Drive East, Los Angeles, CA 90095, USA
[43]Department of Behavioural Neurobiology, Max Planck Institute for Biological Intelligence, Eberhard-Gwinner-Straße 1, Seewiesen 82319, Germany
[44]Department of Biology, University of Florida, P.O. Box 118525, Gainesville, FL 32611, USA
[45]Department of Wildlife Ecology and Conservation, University of Florida, 110 Newins-Ziegler Hall, Gainesville, FL 32611, USA
[46]Estación de Biodiversidad Tiputini, Colegio de Ciencias Biológicas y Ambientales, Universidad San Francisco de Quito, Diego de Robles S/N y vía Interoceánica, Quito 170901, Ecuador
[47]Department of Biology & Neuroscience Minor, University of Mississippi, 30 University Ave, University, MS 38677, USA
[48]Bird Conservancy of the Rockies, 230 Cherry Street, Suite 150, Fort Collins, CO 80521, USA
[49]Smithsonian Conservation Biology Institute, Migratory Bird Center, 3001 Connecticut Avenue NW, Washington, DC 20008, USA
[50]Department of Biology, Millersville University, P.O. Box 1002, Millersville, PA 17551, USA
[51]Department of Integrative Biology and Physiology, University of California, Los Angeles, 610 Charles E. Young Drive East, Los Angeles, CA 90095, USA
[52]Smithsonian Tropical Research Institute, Luis Clement Avenue, Building 401, Tupper, Ancon, Panama City 0843-03092, Panama
[53]Department of Ecology, Evolution, and Organismal Biology, Brown University, 171 Meeting St, Providence, RI 02912, USA
[54]Bond Life Sciences Center, Department of Animal Sciences, Department of Surgery School of Medicine, Institute for Data Science and Informatics, University of Missouri, 1201 Rollins Street, Columbia, MO 65211, USA

*(Affiliations continued on next page)*

Current Biology
Article

CellPress
OPEN ACCESS

John G. Blake,[45,46] Lainy B. Day,[47] T. Brandt Ryder,[48,49] Ignacio T. Moore,[35] Brent M. Horton,[50] Barney A. Schlinger,[41,51,52] Matthew J. Fuxjager,[53] Wesley C. Warren,[54] Emily H. DuVal,[55] W. Alice Boyle,[16,56] Bette A. Loiselle,[45,46,57] Michael J. Braun,[3,18] and Maude W. Baldwin[6,59,*]

[55]Department of Biological Science, Florida State University, 319 Stadium Drive, Tallahassee, FL 32306, USA
[56]Department of Biology, University of Western Ontario, 1151 Richmond Street, London, Ontario N6A 3K7, Canada
[57]Center for Latin American Studies, University of Florida, 319 Grinter Hall, Gainesville, FL 32611, USA
[58]These authors contributed equally
[59]Lead contact
*Correspondence: christopher.balakrishnan@gmail.com (C.N.B.), toda.y.e867@m.isct.ac.jp (Y.T.), maude.baldwin@bi.mpg.de (M.W.B.)
https://doi.org/10.1016/j.cub.2026.05.021

of many manakin species perform at "leks" comprising several display sites at which males perform individually or in coordinated groups.[3,4] Manakin displays feature elements not seen in any other birds, including high-speed backflips, aerial leapfrogs, and loud sonations produced mainly by the wings.[5–10] To accomplish these feats, manakins have evolved specialized features such as coordinated multi-male displays,[11] "superfast" muscles,[12] and modified bones and feathers,[13] and they exhibit changes to heart morphology and gene expression profiles, permitting bursts of extreme heart rate elevation.[12,14] Females observe male dances to select copulation partners, then perform all aspects of parental care, from nest building to incubation to chick provisioning, on their own.[15–17] The resulting potential for extreme skew in male reproductive success[16,17] produces classic conditions for sexual selection to shape manakin biology.

Unlike many other suboscine birds, manakins are specialized frugivores (Figure 1C). The consumption of energy-rich fruits has been hypothesized to contribute to the establishment of highly skewed mating systems in multiple ways. In tropical systems, fruits provide conspicuous and abundant food resources year-round.[18] High-fruit diets rich in sugars and lipids may therefore provide sufficient energy resources for females to provision nestlings without assistance, thereby reducing the costs of uniparental care.[3] Energy-rich fruits may also provide the necessary fuel to sustain costly behavioral displays.[19] A complementary hypothesis suggests an important role for spatial clustering of fruit resources in the development of leks (the "hotspot" hypothesis).[19–22] Although a connection between frugivory and sexual selection has long been suggested and was recently highlighted in a large-scale study of the ecological drivers of sexual selection across birds,[23] there is no existing data linking changes in diet and breeding system with the underlying genetic and physiological transitions facilitating the elaboration of traits such as courtship display.

To understand the causes and consequences of sexual selection in the diversification of manakins, we generated genome assemblies for five lek-mating species in the Pipridae family (Figure 1D; Video S1) and leveraged existing population datasets. Four of these species, *Manacus vitellinus*, *Corapipo altera*, *Pipra filicauda*, and *Lepidothrix coronata*, are members of the Piprinae clade, characterized by sexual plumage dimorphism and extreme display behavior. The fifth species, *Neopelma chrysocephalum*, represents the tyrant-manakins (Neopelminae), a clade sister to Piprinae characterized by less complex display behavior and absence of sexual dichromatism. We then integrated genomic analyses and functional testing with comparative analyses of shifts in diet and breeding systems to gain insight into the evolution of the manakin radiation.

## RESULTS

### Genomic signatures of reproductive skew in manakins

Genetic diversity on the sex chromosomes and autosomes is differentially influenced by sex-specific aspects of life history[24,25] and multiple evolutionary forces.[26] Under neutral evolution, the Z chromosome in birds (and X in mammals) has ¾ the effective population size of autosomes and therefore should have ¾ of the genetic diversity of the autosomes. Sexual selection, when characterized by a high variance in male reproductive success, reduces the effective population size of males and the amount of genetic diversity passed on across generations.[26] This reduction of genetic diversity is predicted to be more pronounced on the Z chromosome because male birds carry two copies of Z, whereas females have one. As a result, sexual selection on males should reduce nucleotide diversity of the Z chromosome relative to autosomes (Z/A diversity ratio) below 0.75.[26] A previous study that tested for an association of mating systems with the Z/A ratio in birds[27] using a PCR-based strategy found evidence for a reduced Z/A diversity ratio among lekking compared with non-lekking shorebirds. As the relationship between Z/A ratios and social systems has not yet been examined in other avian clades that differ in mating system (and has also not been examined using whole-genome data) we were curious if a difference in diversity on the Z chromosome would be detectable in manakin genomes.

To examine the effect of a polygynous lek-mating system on sex-linked genomic diversity, we estimated the Z/A ratio for each of the manakin species for which we assembled genomes as well as for two primarily monogamous, non-manakin suboscine passerines, *Empidonax alnorum* ($n$ = 13) and *Rhegmatorhina berlepschi* ($n$ = 11). We estimated genetic diversity for the Z chromosome relative to each of the 14 largest autosomes (>20 MB) using restriction-site-associated DNA sequencing (RAD-seq) data for males (ZZ) of each species (Figure 1E). We predicted that the two suboscine outgroups would have the highest Z/A ratio and the five manakins would have a Z/A ratio below the neutral expectation of 0.75 (dashed line in Figure 1E). Consistent with this prediction, the median Z/A ratios for *R. berlepschi and E. alnorum* were 0.74 and 0.81, respectively, whereas all five manakins had median Z/A ratios below 0.75 (*P. filicauda* [$n$ = 2, Z/A = 0.65], *C. altera* [$n$ = 33, Z/A = 0.58], *L. coronata* [$n$ = 6, Z/A = 0.54], *M. vitellinus* [$n$ = 20,

Please cite this article in press as: Balakrishnan et al., Genomic and physiological changes in a sexually selected and frugivorous bird radiation, Current Biology (2026), https://doi.org/10.1016/j.cub.2026.05.021



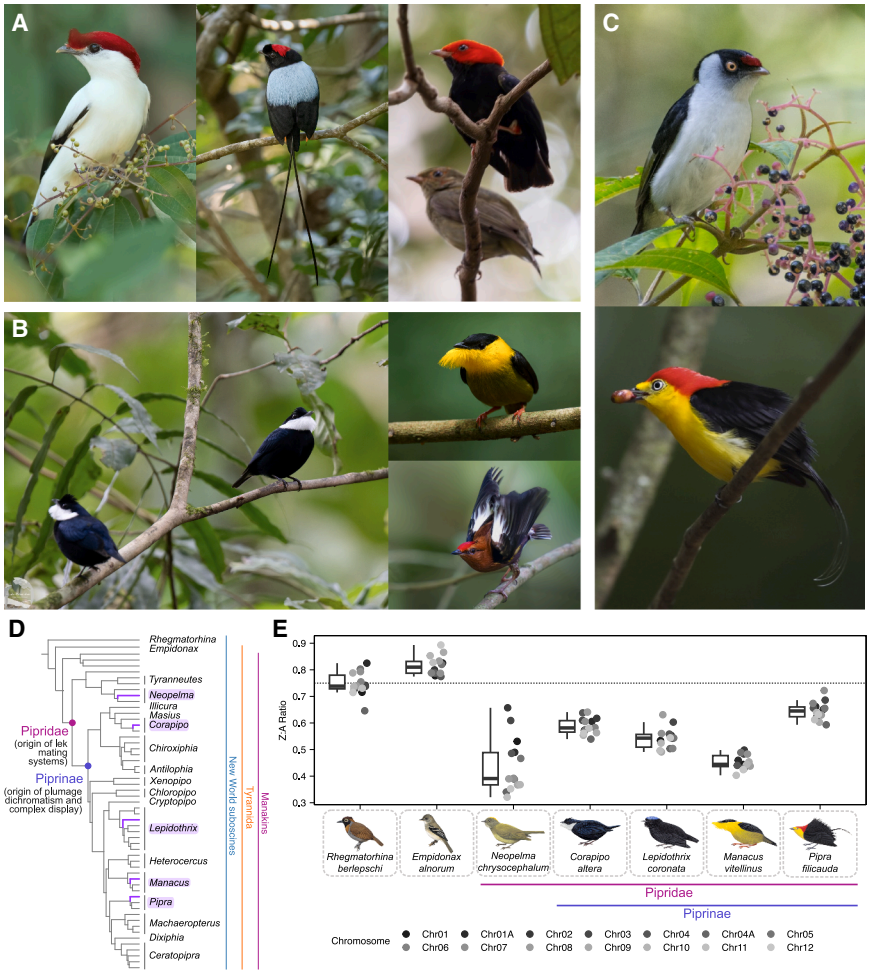


**Figure 1. Signatures of sexual selection in manakin genomes**

(A–C) Many manakin species exhibit striking and dimorphic plumage (photos accessioned into the Cornell Lab of Ornithology | Macaulay Library; all images of male manakins unless otherwise noted: (A, Araripe manakin [*Chiroxiphia bokermanni*] ML624113395 [Photographer: Lev Frid]; long-tailed manakin [*Chiroxiphia linearis*], ML550961471 [Hans Petermann]; red-headed manakin [*Ceratopipra rubrocapilla*] male and female, ML609637328 [Gabriel Bonfa]) as well as coordinated display behavior (B, white-ruffed manakin [*Corapipo altera*], ML545281151 [Alex Molina], golden-collared manakin [*Manacus vitellinus*] ML623044154 [Jeff Hapeman]) and acoustic components facilitated by modified plumage or skeletal morphology (B, bottom right, club-winged manakin [*Machaeropterus deliciosus*], ML616799104 [Jean Bonilla]). In addition, manakins are highly frugivorous (C, pin-tailed manakin [*Ilicura militaris*] ML523242101 [Marcos Eugênio]; wire-tailed manakin [*Pipra filicauda*] ML204131241 [Anselmo d'Affonseca]), which has been hypothesized to facilitate energy-intensive displays and potentially to contribute to lekking behavior.

(D) Cladogram of genera in the Pipridae family and two suboscine outgroups, and purple shading indicates the phylogenetic position of five newly sequenced manakin species.

(E) The ratio of genetic diversity on the Z chromosome is less than the neutral expectation of 0.75 in all five manakins examined. Depicted are RAD-seq estimates of the ratio of Z chromosome to autosomal diversity for the 14 largest autosomes. Dots indicate the individual Z/A ratios, depicted in varying shades of gray. Boxplots illustrate median and 25$^{th}$, 50$^{th}$, and 75$^{th}$ percentiles; whiskers extend to data points 1.5 times the interquartile range (IQR). Number of birds sampled: *E. alnorum*: $n$ = 13; *R. berlepschi*: $n$ = 11; *N. chrysocephalum*: $n$ = 7; *C. altera*: $n$ = 33; *L. coronata*: $n$ = 6; *P. filicauda*: $n$ = 2; and *M. vitellinus*: $n$ = 20. Drawings in (E) © Lynx Edicions (non-manakins) and Kristen Orr (manakins).
See also Figure S1 and Video S1.

Z/A = 0.44], and *N. chrysocephalum* [$n$ = 7, Z/A = 0.39]). Qualitatively similar results were obtained across species, regardless of whether the RAD-seq datasets were mapped to each species' own reference genome (or for the outgroups, to the genome of the closest relative) or all datasets were mapped to a single genome assembly (Figure S1). These results are broadly consistent with the theoretical prediction that long-term sexual selection should reduce the Z/A diversity ratio.

Other factors beyond sexual selection likely contribute to the observed Z/A variation among species, including population demography, sex-specific life history, and selective sweeps.[24–26,28] Among these, sex-specific generation times[25] may be of particular importance in manakins, as male generation times are generally longer than females due to the time it takes males to develop definitive adult plumage[29] and acquire display courts.[29,30] Some manakins have age-based queues for social dominance[29] that further increase the ratio of male to female generation times and would be predicted to also increase the Z/A ratio.[25] The sexually dimorphic *P. filicauda* was the only species in our study known to have age-based dominance queues,[29] and it did have the highest median Z/A diversity ratio ($n$ = 2, Z/A = 0.65) of manakins sampled. Further comparative work that controls for life history, selective sweeps and demographic variation among manakin species and populations will clarify the relative influence of these factors.

## Genomic signatures of positive selection and regulatory evolution

We next used alignments of protein-coding genes from our newly sequenced genomes to test for selection prior to and within the manakin radiation (Figures 2A and 2B). In addition, we also examined changes in putative regulatory elements (Figures 2C and S2A–S2D). For the positive selection tests, we used an iterative approach, both due to genome availability and to optimize alignment quality. We first analyzed a ten-species alignment (Figure 2A: five manakins, a single suboscine outgroup to manakins [*Empidonax traillii*], two oscines [*Ficedula albicollis* and *Corvus cornix*], and two non-passerines [the budgerigar *Melopsittacus undulatus* and golden eagle *Aquila chrysaetos*]) and conducted tests of episodic diversifying

Please cite this article in press as: Balakrishnan et al., Genomic and physiological changes in a sexually selected and frugivorous bird radiation, Current Biology (2026), https://doi.org/10.1016/j.cub.2026.05.021



CellPress
OPEN ACCESS

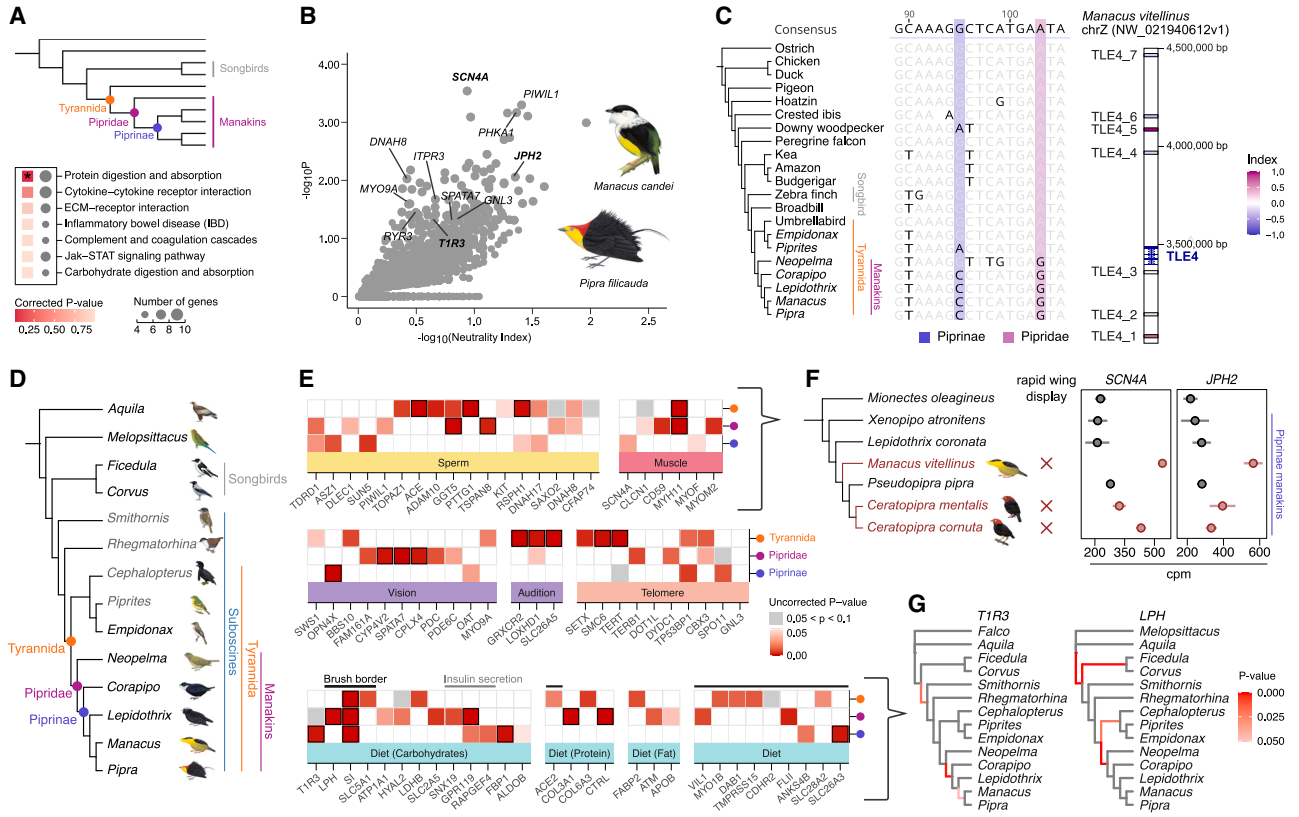


**Figure 2. Tests of positive selection, changes in non-coding regions, and gene expression shifts**

(A) Initial selection tests were performed on alignments of protein-coding genes from 5 manakin species and 5 outgroup species using aBSREL. Positively selected genes in manakins (Pipridae) are significantly enriched in KEGG pathways related to protein digestion (other terms are depicted that were significant [$p < 0.05$] before [but not after] multiple corrections, including carbohydrate digestion and absorption).

(B) MK tests for positive selection were conducted with *M. candei* and *P. filicauda*; a subset of selected genes associated with muscle, diet, sensory, and telomere traits from enrichment analyses are labeled (including three genes, *T1R3*, *SCN4A*, and *JPH2*, in bold, examined below).

(C) Segment of a manakin-accelerated ultraconserved non-coding element (UCNE) proximal to the transcription factor *TLE4*, which plays a role (with MEIS2, see Figures S2A–S2C) in the development of the optic tectum, an avian midbrain area involved in visual motion detection and head-orienting reflexes. Changes in UCNEs proximal to *TLE4* were categorized as occurring either in Pipridae or after the divergence of *Neopelma* (in Piprinae) (positive index values: more changes in Pipridae relative to changes in Piprinae, see also S2D).

(D) Phylogenetic relationships of ten original taxa (in black) together with 4 additional suboscines (in gray) used for additional selection tests and location of three focal nodes for aBSREL testing indicated by colored circles.

(E) Heatmap showing results of positive selection in curated genes related to different biological categories (many flagged in enrichment analyses) (branch models, aBSREL; uncorrected $p$ values; $p < 0.05$ in pink to red, $p = 0.05$–$0.1$ in gray; corrected $p$ values $< 0.05$ indicated with a black outline).

(F) Example of two genes under selection in *Manacus*, which also show evidence of increased expression levels in *Manacus* in the specialized "superfast" forelimb muscle *scapulohumeralis caudalis* (SH) ($n = 3$ samples per species) involved in rapid flight displays (*SCN4A*, *Manacus* and *Ceratopipra*, BayesFactor = 0.44; *JPH2*, *Manacus* only, BayesFactor = 0.61). In both cases, pairwise Tukey tests between *Manacus*, *Lepidothrix*, and *Pseudopipra* were conducted ($p < 0.01$); see STAR Methods. CPM, counts per million; values represent mean ± SE.

(G) Examples of aBSREL results for two candidate genes, *T1R3* and *LPH*, used in subsequent functional tests. Red branches indicate positive selection (uncorrected $p < 0.05$).

Bird images are reproduced with permission from Lynx Nature Books and Cornell Lab of Ornithology and Kristen Orr.

See also Figure S2 and Tables S1–S3.

selection in protein-coding genes at key nodes of the suboscine phylogeny (Figure 2A) using adaptive branch-site random effects likelihood (aBSREL).[31] We then used functional enrichment patterns from these selection tests (Figure 2A; Table S1) to identify candidate genes for a subsequent analysis (Figures 2D and 2E; Table S2) incorporating four additional suboscine genomes that were more recently released. Sampling these additional taxa allowed us to localize selection signatures within the suboscine radiation. We complemented these phylogenetic tests with a population-based McDonald-Kreitman (MK) test[32] using existing whole-genome resequencing data[33] to examine recent positive selection in *Manacus*, a lineage in which extensive work has been done on the physiological basis of complex display[12,34] (Figure 2B).

In the preliminary aBSREL analyses on the 10-species alignment, we observed statistical signatures of positive selection on 1,011 unique, annotated loci across the three focal nodes (suboscines with the Tyrannida clade [653], Pipridae [301], and Piprinae [155]) out of 9,436 alignments. Additionally, in the MK test, 113 annotated loci showed evidence of selection in the

Please cite this article in press as: Balakrishnan et al., Genomic and physiological changes in a sexually selected and frugivorous bird radiation, Current Biology (2026), https://doi.org/10.1016/j.cub.2026.05.021



*Manacus* lineage. To determine whether some gene functions were common targets of selection, we tested for functional enrichment among these gene sets and across these key nodes using Gene Ontology (GO), Uniprot, and Kyoto Encyclopedia of Genes and Genomes (KEGG) databases in the Database for Annotation, Visualization and Integrated Discovery(DAVID.[35,36]). Across all aBSREL analyses, only ''protein digestion and absorption'' showed significant enrichment after correction for multiple testing (Figure 2A; adjusted $p = 0.02$, 5.73-fold enrichment, 9 positively selected genes), and this was significant at the Pipridae node, suggesting that diet-related genes might be a key axis of molecular adaptation in manakins. Three immune-related terms, as well as the GO term ''blood microparticle,'' were also significantly enriched in the MK test gene set. Weaker enrichment (between 2- and 40-fold enrichment, uncorrected $p < 0.1$) was also observed for several functions potentially related to sexual selection (e.g., Pipridae: sarcolemma [muscle], $p = 0.03$, 6 genes under selection; suboscine: vision, $p = 0.04$, 10 genes; Piprinae: chromosome, telomeric region, $p = 0.02$, 4 genes; MK test: spermatid development, $p = 0.08$, 3 genes) and diet (e.g., suboscine: brush border, $p = 0.1$, 8 genes; Pipridae: carbohydrate digestion, $p = 0.04$, 4 genes). We used genes associated with these functional terms as candidate gene lists (Table S2) for further examination.

After incorporating four additional suboscine taxa for the candidate genes, selection signatures were retained in many diet-related genes both on the Pipridae branch and the earlier Tyrannida branch (leading to the clade including manakins, cotingas, and tyrant flycatchers; Figures 2D and 2E), continuing in some cases throughout the manakin radiation (Figure 2E). Some of these genes were associated with sensing and metabolizing sugars, including intestinal carbohydrate transporters (*SLC5A1* and *SLC2A5*) and fructose-1,6-bisphosphatase (*FBP1*), an enzyme involved in glycolysis and gluconeogenesis that was strongly selected specifically in the branch leading to Piprinae. In addition, selection signals were also seen in the taste receptor *T1R3* (Figures 2B, 2E, and 2G), in sucrase-isomaltase (*SI*) (the primary intestinal disaccharidase responsible for breaking sucrose into glucose and fructose), as well as in other loci associated with the brush-border membrane of the intestine and in loci associated with insulin secretion.

Unexpectedly, the dissaccharidase lactase, also known as lactase-phlorizin hydrolase (encoded by the gene *LCT*, also called *LPH*), also showed a strong signature of selection (Figures 2E and 2G). In addition to hydrolyzing sugars such as lactose, lactase-phlorizin hydrolase (hereafter, ''LPH'') also hydrolyzes glycosyl ceramides and dietary (iso)flavonoid glycosides, as well as other diverse glycosides,[37,38] some of which are toxic and are found as secondary compounds in chemically defended fruits. This same enzyme provides a textbook example of adaptive evolution in humans, where its expression is associated with consumption of breast milk and restricted to childhood in many populations, leading to ''lactose intolerance'' in most human adults. Interestingly, persistent expression of LPH has evolved convergently in multiple pastoral populations,[39] allowing adults to consume large quantities of dairy products, which are rich in lactose. However, many questions regarding the primary ancestral role of LPH in non-mammalian vertebrate clades (such as birds) remain unanswered.

We also observed selection on multiple telomere-related genes (Tables S1 and S2; Figures 2B and 2E). As in the diet-related genes, telomere signatures were observed deeper in the tree (Figure 2E) as well as in the *Manacus* lineage (Figure 2B). This signature may relate to long lifespans, which have been observed in many tropical birds, including tropical suboscines,[40] and in manakins specifically (up to 18 years).[41] In manakins, selection on telomere function may also be an evolutionary response to cumulative physiological stress associated with lekking behavior: recent studies of territorial and ''floater'' male *P. filicauda* found evidence of up-regulation of telomere maintenance genes in territorial males[11] and faster attrition of telomeres in more highly cooperative males.[42]

In addition, we observed positive selection on genes possibly involved in the perception and generation of elaborate displays. Loci under positive selection included sensory genes related to vision (Figure 2E)[43,44]: melanopsin (*OPN4X*), other components of the phototransduction cascade (*PDC* and *PDE6C*), and six other vision-related genes that showed selection signatures in manakins, suggesting that visual system changes accompanied the transition to complex displays. Although some manakins, including *Manacus*, do produce unusual sounds in their displays (Video S1), selection signatures on auditory genes were generally weak and deeper in the tree. Finally, several genes related to muscle performance, which is known to be enhanced in some manakin lineages, showed signatures of selection (Figures 2B, 2E, and 2F). Previous work identified key expression changes associated with rapid wing displays and enhanced muscle performance in *Manacus* and *Ceratopipra* manakins.[12] We identified a set of four genes that were significant in the MK test and showed evidence of expression change in scapulohumeralis (SH) muscle, the key muscle modified in *M. vitellinus* for these displays.[45] Of these four genes, *JPH2* and *SCN4A* encode proteins with functions related to myocytic depolarization and calcium flux in muscle. Although previous work[12] found that amino acid sequence and expression changes were largely decoupled, here we identify cases in which changes to both the sequence and the expression may contribute to altered muscle physiology in *Manacus* (Figures S2E and S2F).

In addition to the selection tests, we tested for accelerated divergence among a set of ultraconserved non-coding elements (UCNEs; Figures 2C and S2D; Table S3) to identify potential regulatory changes in manakins. We identified a set of 99 UCNEs (out of 4,351) with significant sequence divergence in manakins relative to other avian genomes (Table S3). Manakin-divergent UCNEs were proximal to genes enriched for functional terms associated with transcriptional regulation (Table S3), suggesting that changes to these UCNEs in the manakin lineage could affect the expression of key transcription factors and therefore influence several phenotypes. Some UCNEs formed clusters around important transcription factors, in particular *NR2F1* with 10 and *TLE4* with 7 proximal manakin-divergent UCNEs. Both of these were associated with more manakin-divergent UCNEs than would be expected by a randomization test of the UCNE set (adjusted $p < 0.05$). Like some of the positively selected protein-coding genes discussed above, both NR2F1 and TLE4 are known to be involved in the development of the visual system,[46,47] along with several other genes adjacent to manakin-divergent UCNEs, including *MEIS2*, *PAX6*, *PBX3*, *POU6F2*, and *ISL1* (see Table S3). Interestingly, TLE4 and MEIS2 are known to interact in the development of the

Please cite this article in press as: Balakrishnan et al., Genomic and physiological changes in a sexually selected and frugivorous bird radiation, Current Biology (2026), https://doi.org/10.1016/j.cub.2026.05.021



CellPress
OPEN ACCESS

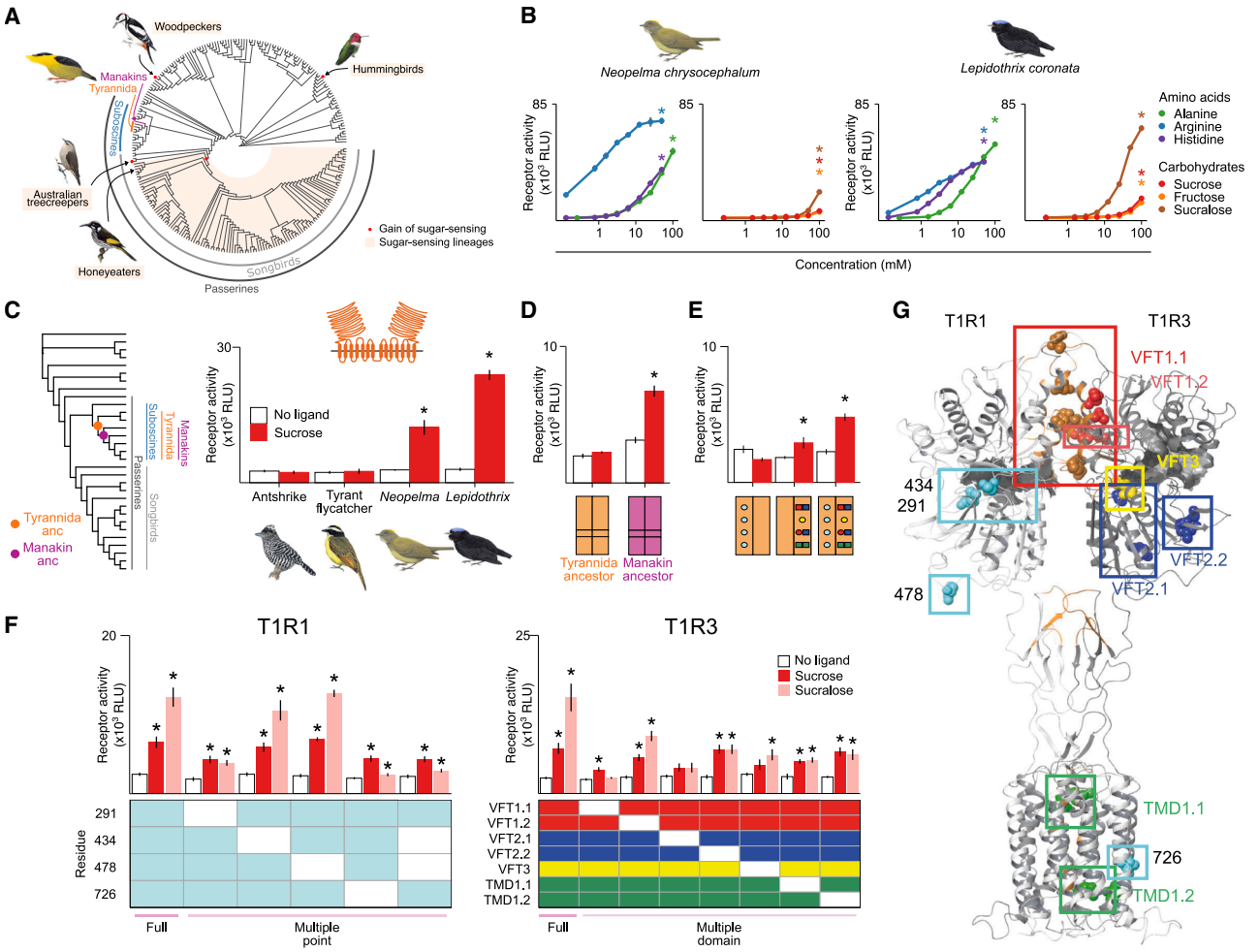


**Figure 3. Molecular basis of sugar detection by manakin taste receptors**

(A) Illustration of independent origins of sweet sensing in birds. Family-level bird tree (from Toda et al.[51]) with locations of lineages with sugar-responsive T1Rs (including hummingbirds,[50] woodpeckers,[52] and many songbirds[51]); the phylogenetic position of manakins (purple) is indicated.

(B) T1R1-T1R3 from two manakin species respond to both amino acids as well as sugars and sweeteners. Dose-response curves from transfected cells expressing taste receptors from two manakin species, the saffron-crested tyrant manakin (*Neopelma chrysocephalum*) and the blue-crowned manakin (*Lepidothrix coronata*) ($n = 6$ replicates per concentration, mean ± SE; differences between highest and lowest concentration, $p < 0.01$, Welch's one-tailed $t$ test).

(C and D) Two ancestral taste receptor heterodimers were reconstructed; topology depicts relationships of taxa used in the reconstruction. Sugar response of T1R1-T1R3 to 100 mM sucrose and no-ligand control from two non-manakin suboscines, an antshrike (*Thamnophilus doliatus*) and a rusty-margined flycatcher (*Myiozetetes cayanensis*)[51] (C) are shown for comparison. Reconstructed receptors (D) from the manakin ancestor, but not the Tyrannida ancestor, respond to sugar (<0.05, Welch's one-sided $t$ test compared with no-ligand controls, mean ± SE).

(E–G) Chimeric dissection (E and F) and homology modeling (G) uncovers 22 important residues in T1R1 and T1R3 (< 0.05, Welch's one-sided $t$ test compared with no-ligand controls; false discovery rate [FDR] correction for multiple testing, mean ± SE; see Figure S3 for analysis of critical residues combinations). Brown T1R3 residues and brown shaded regions are at the interface with (within 4 angstroms of) the other heterodimer. Receptor activity is calculated as the area under the curve (AUC) and is expressed as relative light units (X10$^3$ RLU).

Bird images are reproduced with permission from Lynx Nature Books and Cornell Lab of Ornithology and Kristen Orr.

See also Figure S3.

tectum, a brain region critically involved in motion detection in the visual processing pathway and head/eye orienting responses, which has been implicated, among other things, in visual attention, decision-making, and prey capture.[46,48,49]

## Functional changes in taste receptors

We were interested in the positive selection signals in genes associated with diet, such as loci involved in taste and digestion, and we next sought to examine whether these signals reflected actual changes in protein function. First, we examined the taste receptor T1R3, a receptor in which our previous work had documented convergent functional changes in multiple clades of birds, including nectar-taking, frugivorous, and sap-feeding taxa. Birds have lost the gene encoding the sweet receptor subunit *T1R2* required by mammals to detect sugar. Instead, in hummingbirds, songbirds, and woodpeckers,[50–52] the savory receptor (T1R1-T1R3) has been repurposed to detect sugars as well as amino acids (Figure 3A). Functional changes are not

Please cite this article in press as: Balakrishnan et al., Genomic and physiological changes in a sexually selected and frugivorous bird radiation, Current Biology (2026), https://doi.org/10.1016/j.cub.2026.05.021



always reflected in positive selection signatures: we had previously documented functional shifts in T1Rs in some clades of birds at points in the phylogeny that did not show evidence of selection (see Toda et al.)[51]; therefore, we were very interested in the clear selection signature present in T1R3 at the Piprinae node (Figures 2E and 2G) and in the *Manacus* MK test (Figure 2B). Manakins often swallow fruit whole and have been thought to rely less on taste than other frugivores—a previous comparison of two manakin species (*Pipra mentalis* and *Manacus candei*) did not document a preference for sweetened diets.[53] We cloned taste receptor sequences (T1R1 and T1R3) from two manakins, two outgroups, and two ancestral node reconstructions into expression vectors and tested the responses of the expressed proteins to sugars and amino acids *in vitro* with a cell-based luminescence assay (Figures 3B–3D). These tests indicate that manakins (like hummingbirds, woodpeckers, and most songbirds) have also re-evolved T1R-based sugar sensing from a sugar-insensitive ancestor. Interestingly, the ability to respond to sugar is already present in *Neopelma* and in the reconstructed common ancestor of all manakins but is absent from the common ancestor with tyrannids (Figure 3D).

Extensive chimeric dissection (Figures 3E, 3F, and S3) of the two ancestral taste receptor pairs revealed a critical role of 22 residues in the response to sucrose and sucralose (Figures 3F, S3A, S3D, and S3E). Strikingly, the majority of changes are in T1R3, including in the Venus flytrap region (VFT), which is modified in hummingbirds to enable sugar binding (Figures 3G, S3B, and S3C). By contrast, songbirds, although more closely related to manakins, modify the VFT of T1R1, underscoring the independent origin of each sugar-sensing gain. Similar to residues in songbird T1R1, many critical residues in the VFT of manakin T1R3 are found at the interface between the receptors (Figure 3G; T1R3 residues in VFT1.1 as well as receptor regions colored brown are within 4 angstroms of the other heterodimer). Chimeric analysis confirmed the necessity and sufficiency of the different domain regions in T1R3 and highlighted a critical role of a small number of residues in T1R1 (Figures 3G and S3A). Unlike in other sweet-sensing birds, we uncovered important changes in the binding pockets of both receptors (Figures S3B and S3C), as well as in both transmembrane domains. Manakins therefore recruit the same ancestral receptor pair to sense sugars employed by other nectar-taking birds, but the functional change is effected by different underlying residues.

## Functional changes associated with fruit digestion

As suggested by the positive selection tests, specialized frugivores such as manakins likely also exhibit changes in digestive systems—in addition to sensory changes—that enable them to consume fruits. Fruits vary extensively in chemical composition across species and can be rich in sugars as well as lipids.[54] In addition, many fruits contain secondary metabolites, some of which can serve as defense compounds.[55] Manakins are important seed dispersers and consume fruits from diverse plant species[54,56–58] (Figures S4A–S4C). Interestingly, some manakins also have been observed to consume unripe fruits (that are often protected by toxic compounds) either frequently[56] or when ripe fruits are not available.[58] It has been hypothesized that frugivorous birds may be able to ingest otherwise toxic fruits by passing glycosides without rendering them active by hydrolysis[59]; however, how manakins deal with dietary toxins is not known.

We found signatures of selection in genes encoding enzymes related to glycoside digestion. For example, positive selection signals were seen in *ATP1A1*, a multifunctional enzyme with roles in muscle contractility[60] as well as in digestion, conferring resistance to toxic glycosides—closer examination revealed manakin-specific changes at residues (including site 122) known to reduce toxin sensitivity in both insect herbivores and frogs.[61,62] In addition, we also observed strong signatures of selection on *LPH* (Figures 2E and 2G), the gene encoding lactase-phlorizin hydrolase (also known as ''lactase,'' see above). LPH encodes a β-glucosidase digestive enzyme with a role in glycoside hydrolysis; in RNA sequencing (RNA-seq) data of intestinal tissue from golden-collared manakins, we observed *LPH* expression, albeit at low levels (Figures S4D and S4E). In mammals, LPH is involved in breaking down β-linked disaccharides such as lactose, using the second active site. However, as a bifunctional enzyme with two functional subunits, LPH is also involved in hydrolyzing glycosides (such as phlorizin, hydrolyzed primarily using the first active site but also by the second site[38,63]), many of which are toxic plant secondary metabolites.[37] Amygdalin, a cyanogenic glycoside in fruit, was nontoxic to frugivorous cedar waxwings,[59] and studies of enzymatic activity from intestinal homogenates failed to document appreciable activity against lactose in chickens,[64] and against both lactose and amygdalin in house sparrows and frugivorous bulbuls,[37] leading to the proposal that reduced *LPH* expression was one mechanism that could permit toxic fruit to be consumed. We were therefore curious if the signature of selection on *LPH* in manakins could be related to reduced functionality of this enzyme.

To investigate whether the selection signature on lactase reflected functional changes within manakins, we synthesized the coding sequence of *LPH* orthologs from manakins and outgroups and examined their hydrolytic activity in cell-based functional assays (Figure 4). These assays are the first to demonstrate lactase activity (or glycoside hydrolysis) in birds and show distinct evolutionary patterns of catalytic activity against the two substrates. Whereas chicken LPH is catalytically active against both lactose and phlorizin and flycatcher LPH is catalytically active against lactose, the functionality of manakin orthologs against both substrates, although still generally higher than controls, was markedly reduced (Figure 4A). Functional testing of ancestrally reconstructed proteins demonstrated that phlorizin hydrolysis was reduced prior to the manakin radiation in the ancestor of Tyrannida (relative to the previous suboscine node) (Figure 4B), whereas a regain of function against lactose (low in both the suboscine and the Tyrannida ancestor) was observed in the rusty-margined flycatcher *Myiozetetes cayanensis* (Figure 4A). A similar reduction was found in both lactase and phlorizin in the chicken (Figure 4A) compared with the neognath ancestor (Figure 4B): like in manakins, chickens (and also songbirds) appear to have convergently evolved functional reductions (relative to the neognath and passerine ancestors, respectively) (Figure 4B). We next tested whether these functional shifts were consistent with selection signatures. Interestingly, the functional reduction does not appear to be due to relaxed selection but rather to intensified positive selection in all four groups (galliforms, songbirds, manakins, and the clade consisting of

Please cite this article in press as: Balakrishnan et al., Genomic and physiological changes in a sexually selected and frugivorous bird radiation, Current Biology (2026), https://doi.org/10.1016/j.cub.2026.05.021



CellPress
OPEN ACCESS

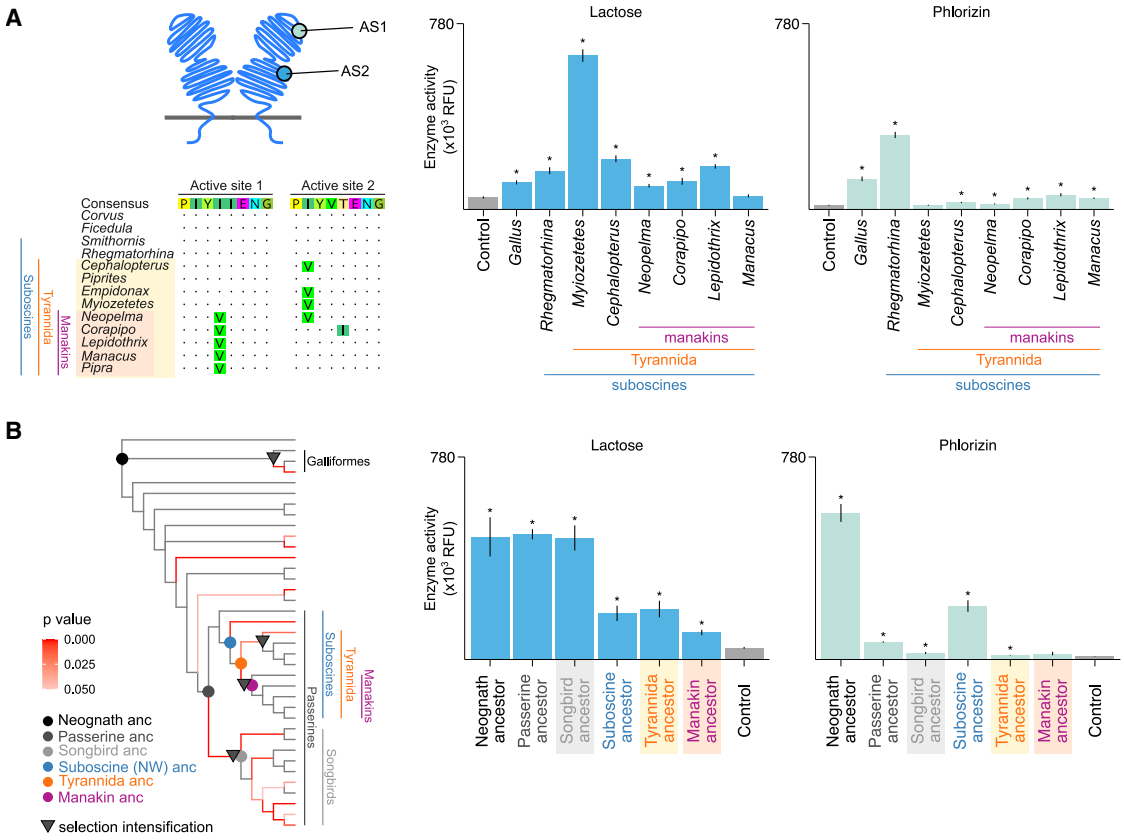


**Figure 4. Reduction in function of lactase-phlorizin hydrolase in manakins**

(A) Left: schematic of the structure of the β-glucosidase digestive enzyme lactase-phlorizin hydrolase (LPH) with the location of active sites, and substitutions in manakin and other Tyrannida active sites (as well as a substitution to M in the second position of the first active site in chicken and quail, not shown) suggest possible functional variation. Activity (right) of LPH from eight bird species as well as untransfected control cells (gray) is assessed by monitoring glucose levels after incubation with lactose (66.6 mM) and phlorizin (1.67 mM): whereas the tyrant flycatcher (*Myiozetetes cayanensis*) had the highest activity against lactose, and the chicken and antbird had the highest phlorizin activity, the activities of all manakin enzymes (against both substrates) are reduced (but most are still significantly greater than untransfected controls; $^{*}p < 0.05$, $n = 9$ replicates per substrate, Welch's one-sided $t$ test relative to controls, FDR correction, mean ± SE). Enzymatic activity is calculated as the area under the curve (AUC) and is expressed as relative fluorescence units ($X10^3$ RFU).

(B) Topology used for ancestral reconstruction of avian LPH. Red branches indicate results of positive selection testing (red: uncorrected $p < 0.05$ with aBSREL). Triangles indicate the location of selection intensification (instead of relaxation, tested with RELAX) observed at the ancestor of manakins, the ancestor of tyrants and cotingas, the ancestor of songbirds, and of the galliforms (Cotingidae and Tyrannidae: average K = 4.39; Pipridae: K = 3.27; Passerines: K = 3.68; Galliformes: K = 2.26; at least 9 of 10 runs were significant [$p < 0.05$]). Functional testing of reconstructed ancestors shows a pattern of reduced activity (against both substrates) in both the manakin ancestor and the ancestor of Tyrannida. In (B), "suboscine ancestor" refers to the ancestor of New World (NW) suboscines (after divergence from Old World suboscines). A convergent reduction against phlorizin is also seen in songbirds (gray shading).

See also Figure S4.

cotingas and tyrants [Figure 4B]). In addition, three of these four lineages also had substitutions in the active sites (Figure 4A), but reversing these changes alone did not recover activity: there was no significant difference in function between wild-type LPH and one-point (chicken, *Myiozetetes*, and *Neopelma*) or two-point active-site mutants (*Neopelma*) ($n = 6$, Welch's two-tailed test), implicating the contribution of other residues outside of the active sites in the change in function. Similar to avian capsaicin insensitivity, which enables birds to consume fruits of chillies (*Capsicum*) (and plants to select for preferred seed dispersers),[65] reduced LPH activity may have evolved to render frugivores such as manakins immune to the toxicity of dietary glycosides in fruit.

In addition to enabling toxic glycosides in fruit to be passed, reduced LPH function could also be related to the effect of some glycosides in decreasing the activity of sugar transporters. Some transporters, including some GLUT transporters, are inhibited by phloretin, the byproduct of phlorizin hydrolysis. *SLC5A1*, the gene encoding an important transporter also involved in rapid post-ingestive responses to sugar, is under selection in Piprinae manakins (Figure 2E) and is also inhibited by phlorizin in some species.[66] By decreasing LPH activity and potentially through modifying activities or functions of sugar transporters, manakins may reduce the inhibition of sugar transport, allowing more energy to be made available. Many questions about avian LPH remain: investigating the role of lactase in non-frugivores (as well as in other non-mammalian vertebrates) remains an interesting topic for future research.

Please cite this article in press as: Balakrishnan et al., Genomic and physiological changes in a sexually selected and frugivorous bird radiation, Current Biology (2026), https://doi.org/10.1016/j.cub.2026.05.021



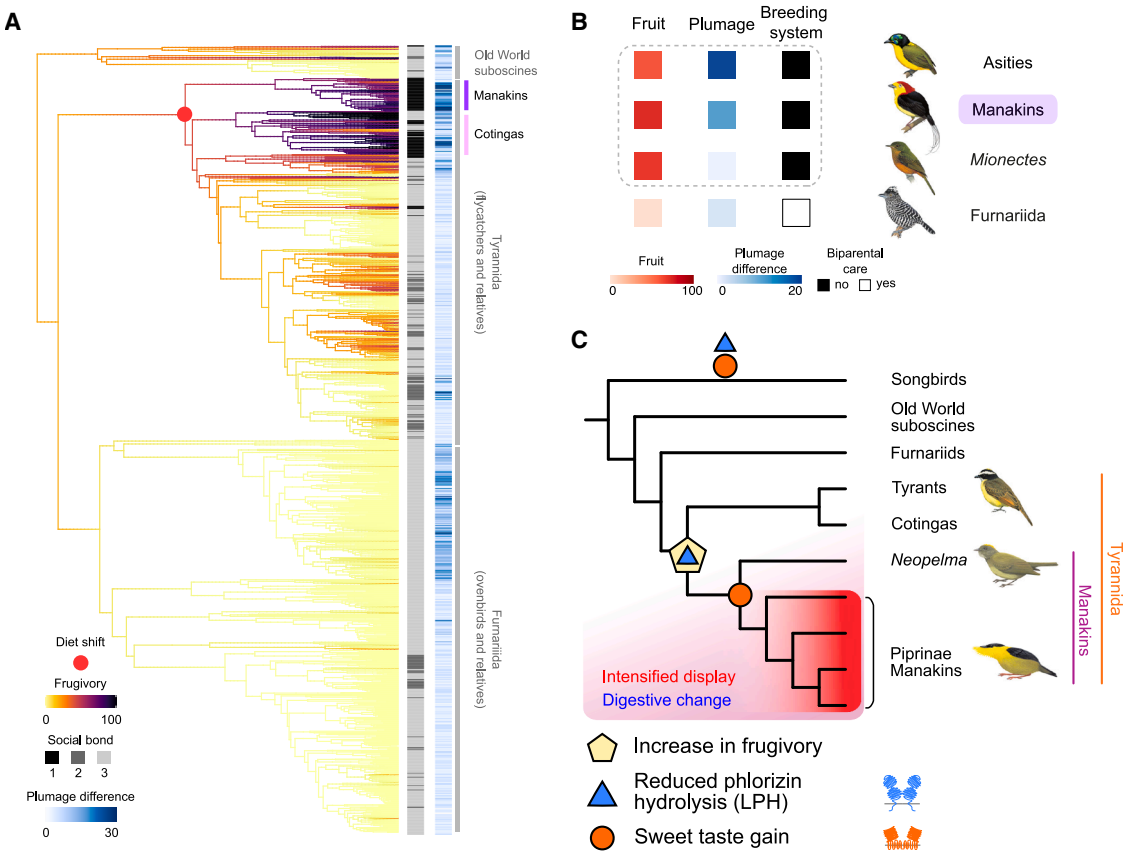


**Figure 5. Diet shifts in suboscines and timing of digestive and sensory changes**

(A) Amount of dietary fruit mapped across the suboscine phylogeny (purple, strongly frugivorous lineages). Variation in social bond (1 = no bond/lekking, 2 = partial bond, and 3 = strong bond/monogamous) and metric of plumage dichromatism across suboscines. The circle indicates the predicted location of an early major diet shift toward intensified frugivory (see Figure S5).

(B) Dietary fruit is associated with shifts in breeding systems across suboscines. Asities (Old World suboscines), manakins, and a genus of lekking tyrant flycatchers (*Mionectes*) are the three most well-supported clades inferred to have lost biparental care coincident with a shift in the inferred optimum of frugivory or plumage dichromatism (see STAR Methods; Figure S5; Table S4). Bird images reproduced with permission from Lynx Edicions.

(C) Model of key changes in the manakin radiation: digestive and sensory changes (some convergent with changes in songbirds) precede the evolution of elaborate displays and courtship behavior.

Bird images reproduced with permission from Lynx Nature Books and Cornell Lab of Ornithology; *N. chrysocephalum* and *M. vitellinus* image © Kristen Orr. See also Figure S5 and Table S4.

## Predicted timing of dietary and breeding system changes

Given the observed genomic changes as well as the specific functional shifts in taste receptors and digestive enzymes, we next examined when the extreme frugivory exhibited by manakins may have evolved—also in relation to other traits such as lek-mating systems, plumage dichromatism, and elaborate display behavior. We surveyed comprehensive databases containing natural history information for suboscines for this information and mapped it onto a recent phylogeny of suboscines.[67–70] Suboscines are a massive radiation of over 1,300 bird species that, together with their sister radiation of songbirds (oscines), form most of the passerine clade that collectively makes up over half of the species of living birds today. Most suboscines are Neotropical and consist of two major groups, the insectivorous Furnariida and the Tyrannida, including tyrant flycatchers, manakins, and cotingas (Figure 5). We observed a marked intensification of frugivory in manakins and cotingas that was subsequently lost in many tyrants and is absent in the entire furnaroid radiation (Figures 5A and S5A). This shift toward frugivory (see also Figure S5A) corresponded to the node where we observed a decrease in the phlorizin hydrolysis activity of LPH (Figure 5C).

Manakins and some cotingas also show elevated levels of dichromatism between males and females (a possible proxy for the intensity of sexual selection; i.e., Dale et al.,[68] but see Huang and Rabosky[28]), as well as loss of monogamous pair-bond behavior. Using a comparative model examining evolutionary changes of diet, breeding system, and plumage traits paired with biologically informed simulations (see STAR Methods), we found a significant association between frugivory and shifts in social system and plumage variation across the suboscine phylogeny, which deviated substantially from a scenario in which diet has no effect on the evolution of social system

Please cite this article in press as: Balakrishnan et al., Genomic and physiological changes in a sexually selected and frugivorous bird radiation, Current Biology (2026), https://doi.org/10.1016/j.cub.2026.05.021





and plumage (Figure 5B; see also STAR Methods; Figures S5B and S5C; Table S4). This result, driven by three lekking clades including manakins, asities (Philepittidae), and *Mionectes* flycatchers, suggests an important role for frugivory in the shifts both in breeding systems and in the elaboration of secondary sexual characteristics associated with sexual selection. Moreover, estimates of macroevolutionary optima show that shifts in biparental care are strongly associated with shifts in clade-specific optima defined by distinct levels of frugivory and traits associated with sexual selection (Table S4; Figures S5B–S5D). Whereas some losses of biparental care were, as in manakins, subsequently followed by the development of elaborate male plumage and subdued female plumage, other losses of biparental care were not, as in the genus *Mionectes*. This suggests that a shift to increased frugivory may have facilitated the loss of biparental care and that the loss of biparental care is sometimes followed by the evolution of elaborate plumage and lekking displays.

## DISCUSSION

Long-standing theory predicts that in specialized avian frugivores—in particular in the lekking Neotropical manakins (Pipridae), cotigas (Cotingidae), and birds of paradise (Paradisaeidae)—enhanced sexual selection was facilitated by the ecological transition toward frugivory.[3,18,23,71] In this study, we focused on the manakin radiation and used a diverse set of approaches to examine the temporal sequence of events that may have facilitated intensified sexual selection and the evolution of complex display behavior. We demonstrate that the transition to intensified frugivory occurred early, prior to the radiation of manakins—likely in the ancestor of all Tyrannida—followed by subsequent reversions to a more insect-rich diet in some members of Tyrannidae. This initial transition toward fruit consumption is accompanied by signatures of selection on diverse genes, including digestive genes, which persist across the radiation. We also observe selection signals on genes associated with the production and perception of sexually selected displays throughout the clade, which may correlate with functional changes.

We observe striking changes that may affect the ability of manakin ancestors to taste and digest fruit. Concordant with the early diet shift in the Tyrannida ancestor, we document a clear functional shift in a digestive enzyme, lactase-phlorizin, resulting in a reduction in the ability of glycosides to be hydrolyzed. Following this shift, in the common ancestor of the manakin radiation (Pipridae), we also observe a functional change in the T1R taste receptor system, enabling the perception of sweet taste—similar to convergent gains in sugar sensing that evolved in hummingbirds, songbirds, and woodpeckers. Whether changes in the digestive system, such as shifts in digestive enzyme function, precede changes in sensory receptors in other lineages warrants further investigation.

Interestingly, we document predicted signatures of reproductive skew in patterns of nucleotide diversity in the lek-mating manakins but not in primarily monogamous outgroups, supporting comparative analyses of shifts in parental care. The shift in breeding systems at the base of the manakin radiation was followed later by the evolution of more elaborate, complex displays and colorful and dimorphic plumage in Piprinae manakins. Collectively, these results demonstrate an important role for adaptations that permit exploitation of high-fruit diets in setting the stage for shifts in breeding systems that may then drive the evolution of elaborate, sexually selected behaviors.[3,18]

## RESOURCE AVAILABILITY

### Lead contact

Requests for further information and resources should be directed to and will be fulfilled by the lead contact, Maude Baldwin (maude.baldwin@bi.mpg.de).

### Materials availability

All unique reagents generated in this study are available from the lead contact without restriction.

### Data and code availability

- Genomes, transcriptomes, and RAD-seq data generated for this paper have been deposited in NCBI and are publicly available as of the date of publication.
- Sequences of cloned taste receptors as well as tested ancestral reconstructions of taste receptors and lactase-phlorizin enzymes are available on GitHub (https://github.com/maggieMCKO/manakin) and archived at Zenodo (Zenodo: 18416735).
- All original code has been deposited at https://github.com/periperipatus/ManacusMK, https://github.com/kfpbennett/manakin_za https://github.com/maggieMCKO/manakin, and https://hub.docker.com/r/michaelsbrewer/coats_test and is publicly available as of the date of publication.
- Any additional information required to reanalyze the data reported in this paper is available from the lead contact upon request.

## ACKNOWLEDGMENTS

We thank the Manakin RCN for feedback and support, as well as the Smithsonian Tropical Research Institute in Gamboa, Panama; the Smithsonian Environmental Research Center in Edgewater, Maryland; the Smithsonian Conservation Biology Institute in Front Royal Virginia; and the Fundação Grupo Boticário at the Salto Morato Reserve in Paraná, Brazil, for hosting meetings of the Manakin Research Coordination network. We thank the B10K project for access to suboscine gene annotations; Pat Minx for support with genome assembly; Leslie Calderon and Fábio Jacomassa for helping in the compilation of literature data; Justin Baldwin for statistical advice; Peter Andolfatto, Pablo Oteiza, and the Evolution of Sensory and Physiological Systems lab for discussions; and Emily Wheeler for editorial assistance. Guy Sella and Guy Amster provided helpful discussion of the Z/A ratio. Funding for this work was obtained from the US National Science Foundation awards 1646806 (W.A.B.), 1122180 (L.B.D.), 1353085 (T.B.R., I.T.M., and B.M.H.), 1947472 (M.J.F.), 1457541 (E.H.D., W.A.B., B.A.L., M.J.B., and C.N.B.), 1655683 (R.T.K. and E.L.B.), the National Institutes of Health R03 NS115145 and R24 GM120464 awards (to C.V.M.), the Brazilian Research Council (CNPq) to M.A.P. (#304742/2019-8), the Smithsonian Competitive Grants Program (M.J.B. and H.C.L.), KAKENHI grants from the Japan Society of Promotion of Science (18KK0166 to Y.I.; 20H02941, 22KK0079, 23H02168, and 25H01362 to Y.T.), the International Collaborative Research Promotion Project from Meiji University (to Y.T.), the JST Forest Program (grant Number JPMJFR220C, Japan) (to Y.T.), the Lotte Shigemitsu Prize (to Y.I. and Y.T.), the Smithsonian National Museum of Natural History and the American Ornithological Society (K.F.P.B.), Schmidt Sciences (LLC) via an Eric and Wendy Schmidt AI in Science Postdoctoral Fellowship to Cornell University (E.T.M.) and the University of Michigan (J.S.B.), East Carolina University (C.N.B.), and the Max Planck Society (to M.W.B.). Bird illustrations © Lynx Nature Books and Cornell Lab of Ornithology, reproduced with permission. Illustrated by Hilary Burn: *Rhegmatorhina berlepschi* (male), *Empidonax alnorum*, *Rhegmatorhina hoffmannsi* (male), *Empidonax hammondii*, *Thamnophilus doliatus doliatus* (male). Illustrated by Jan Wilczur: *Manacus candei* (male), *Piprites chloris chloris*, *Pipra filicauda* (male). Illustrated by Ian Willis: *Aquila chrysaetos*, *Dendrocopos major major* (male). Illustrated by Ian Lewington: *Smithornis capensis camarunensis*, *Myiozetetes cayanensis cayanensis*, *Calyptomena whiteheadi* (male).

Please cite this article in press as: Balakrishnan et al., Genomic and physiological changes in a sexually selected and frugivorous bird radiation, Current Biology (2026), https://doi.org/10.1016/j.cub.2026.05.021



Illustrated by John Cox: *Climacteris picumnus picumnus*, *Philepitta schlegeli* (male). Illustrated by Chris Rose: *Cephalopterus ornatus* (male), *Cephalopterus glabricollis* (male). Illustrated by Norman Arlott: *Ficedula albicollis*, *Contopus caribaeus caribaeus*. Illustrated by Richard Allen: *Melopsittacus undulatus* (male). Illustrated by David Quinn: *Corvus corone cornix*. Illustrated by Douglas Pratt: *Calypte anna* (male). Illustrated by Ren Hathway: *Phylidonyris novaehollandiae*. Illustrated by Brian Small: *Mionectes macconnelli macconnelli*.

## AUTHOR CONTRIBUTIONS

M.W.B., Y.T., M.-C.K., M.E.W., R.J.D., P.E.B., E.T.M., D.M.-A., R.B.D., P.B.F., E.H.S., K.F.P.B., H.C.L., R.T.K., E.L.B., L.B.D., T.B.R., I.T.M., B.M.H., B.A.S., M.J.F., W.C.W., E.H.D., W.A.B., B.A.L., M.J.B., and C.N.B. designed research. E.T.M. designed and conducted comparative analyses with input from D.S.C. and M.W.B. L.B.D., T.B.R., B.A.S., W.A.B., and M.J.F. provided samples for genome and transcriptome sequencing; sample preparation and sequencing were conducted by K.F.P.B., H.C.L., and W.C.W. Genome assembly and quality control were conducted by M.W.B., R.B.D., P.B.F., E.H.S., A.Z., C.T., W.C.W., and M.J.B. R.A.B., K.R., T.B.S., C.F.-V., and M.G. provided access to draft genomes for outgroup taxa. E.H.S., K.F.P.B., H.L.A., P.B.F., M.G.B., and C.N.B. determined estimates of genetic diversity. R.B.D. conducted whole-genome alignments; R.J.D., P.E.B., M.I.M.L., M.J.B., and C.N.B. generated genome-wide alignments of protein-coding genes and performed selection tests with manual validation by M.A., C.F.F., J.S.B., K.M.L., H.C.L., A.E.M., S.E.K., N.D.W.C., S.R.F., C.A.C., E.H.D., W.A.B., and K.F.P.B. M.W.B., M.-C.K., M.E.W., R.J.D., and C.N.B. annotated loci from additional suboscines. M.-C.K., P.E.B., and J.B.P. assigned gene names to poorly annotated loci, with input from M.W.B. and C.N.B. P.E.B. and C.N.B. conducted tests of GO enrichment of selected genes and MK tests. M.E.W. designed and conducted UCNE analyses. M.W.B., M.S.B., and C.N.B. performed a calculation of the index of UCNE changes. A.A.N. conducted *in situ* hybridizations, with input from M.E.W. and C.V.M. R.J.D., J.B.P., M.J.F., and C.N.B. analyzed muscle transcriptomes. M.-C.K. and K.R.S. analyzed transcriptomes from intestine, liver, and kidney, with input from M.W.B., P.E.B., and C.N.B. M.A.P. analyzed fruit composition with input from M.W.B. and M.-C.K. M.W.B. and Y.T. cloned taste receptors. M.W.B. performed ancestral reconstruction of taste receptors. Y.T. generated chimeric taste receptors and tested receptor function with assistance from Y.I. Y.T. and M.-C.K. analyzed receptor responses, with input from M.W.B. Y.T. and T.N. performed homology modeling and visualization of critical residues. M.W.B. and D.M.-A. curated LPH predictions and performed ancestral reconstruction of lactase-phlorizin. D.M.-A. cloned lactase-phlorizin expression vectors and tested enzymatic function, with assistance from J.F.C., M.-C.K., and M.W.B. K.R.S. performed tests of positive and relaxed selection on lactase-phlorizin, with input from M.-C.K. and M.W.B. J.F.C. generated LPH point-mutant chimeras. M.-C.K. and D.M.-A. performed statistical analysis of enzymatic function, with input from M.W.B. M.W.B., Y.T., Y.I., A.R.P., C.V.M., J.G.B., L.B.D., T.B.R., I.T.M., B.M.H., B.A.S., M.J.F., E.H.D., W.A.B., B.A.L., M.J.B., and C.N.B. acquired funding. Video data were contributed by M.A., C.A.C., L.B.D., and W.A.B. M.W.B., Y.T., M.-C.K., M.E.W., and C.N.B. designed the figures. M.W.B. and C.N.B. wrote the manuscript, with input from all authors.

## DECLARATION OF INTERESTS

The authors declare no competing interests.

## STAR★METHODS

Detailed methods are provided in the online version of this paper and include the following:


- KEY RESOURCES TABLE
- EXPERIMENTAL MODEL AND STUDY PARTICIPANT DETAILS
  - Bird specimens for genome sequencing
  - Specimens for transcriptomics
  - Population resequencing and RADseq
  - Gene cloning and functional assay samples
  - Tissue samples for in situ hybridization
- METHOD DETAILS
  - Genome sequencing and assembly
  - *Manacus vitellinus*, *Pipra filicauda*
  - *Lepidothrix coronata*
  - *Neopelma chrysocephalum*, *Corapipo altera*
  - Genome annotation
  - Genome alignment and chromosome assignment
  - Genetic diversity and Z/A diversity ratios
  - MK test using resequencing data
  - MK results and muscle expression data
  - Lineage-specific selection tests on genes
  - Refining poorly annotated gene symbols
  - Enrichment of positively-selected genes
  - RNA-seq of liver, kidney, gut, and muscle
  - UCNE analysis
  - Ancestral reconstruction and selection tests
  - *T1R* and *LPH* cloning and functional testing
  - Structural model
- QUANTIFICATION AND STATISTICAL ANALYSIS
  - RNA-seq quantification
  - Permutation test for UCNE–gene clustering
  - Composition of manakin-consumed fruits
  - Lipid intake by bird family
  - T1R/LPH functional statistics
  - Comparative analyses of suboscine traits


## SUPPLEMENTAL INFORMATION

Supplemental information can be found online at https://doi.org/10.1016/j.cub.2026.05.021.

Received: September 29, 2025
Revised: January 30, 2026
Accepted: May 11, 2026

## REFERENCES


1. Andersson, M.B. (1994). Sexual Selection (Princeton University Press). https://doi.org/10.1515/9780691207278.
2. Darwin, C. (1871). The Descent of Man, and Selection in Relation to Sex (D. Appleton and Company). https://doi.org/10.5962/bhl.title.24784.
3. Snow, D.W. (1963). The evolution of manakin displays. Proceedings of the International Ornithological Congress *13*, 553–561.
4. Bradbury, J.W. (1981). The evolution of leks. In Natural selection and social behavior: recent research and new theory, R.D. Alexander, and D.W. Tinkle, eds. (Chiron Press), pp. 138–169.
5. Prum, R.O. (1990). Phylogenetic analysis of the evolution of display behavior in the Neotropical manakins (Aves: Pipridae). Ethology *84*, 202–231. https://doi.org/10.1111/j.1439-0310.1990.tb00798.x.
6. DuVal, E.H. (2007). Cooperative display and lekking behavior of the Lance-tailed Manakin (Chiroxiphia lanceolata). Auk *124*, 1168–1185. https://doi.org/10.1093/auk/124.4.1168.
7. Barske, J., Schlinger, B.A., Wikelski, M., and Fusani, L. (2011). Female choice for male motor skills. Proc. Biol. Sci. *278*, 3523–3528. https://doi.org/10.1098/rspb.2011.0382.
8. Barske, J., Fusani, L., Wikelski, M., Feng, N.Y., Santos, M., and Schlinger, B.A. (2014). Energetics of the acrobatic courtship in male golden-collared manakins (Manacus vitellinus). Proc. Biol. Sci. *281*, 20132482. https://doi.org/10.1098/rspb.2013.2482.
9. Friscia, A., Sanin, G.D., Lindsay, W.R., Day, L.B., Schlinger, B.A., Tan, J., and Fuxjager, M.J. (2016). Adaptive evolution of a derived radius morphology in manakins (Aves, Pipridae) to support acrobatic display behavior. J. Morphol. *277*, 766–775. https://doi.org/10.1002/jmor.20534.

10. Fuxjager, M.J., and Schlinger, B.A. (2015). Perspectives on the evolution of animal dancing: a case study of manakins. Curr. Opin. Behav. Sci. *6*, 7–12. https://doi.org/10.1016/j.cobeha.2015.06.007.

11. Bolton, P.E., Ryder, T.B., Dakin, R., Houtz, J.L., Moore, I.T., Balakrishnan, C.N., and Horton, B.M. (2025). Neurogenomic landscape associated with status-dependent cooperative behaviour. Mol. Ecol. *34*, e17327. https://doi.org/10.1111/mec.17327.

12. Pease, J.B., Driver, R.J., de la Cerda, D.A., Day, L.B., Lindsay, W.R., Schlinger, B.A., Schuppe, E.R., Balakrishnan, C.N., and Fuxjager, M.J. (2022). Layered evolution of gene expression in "superfast" muscles for courtship. Proc. Natl. Acad. Sci. USA *119*, e2119671119. https://doi.org/10.1073/pnas.2119671119.

13. Bostwick, K.S., and Prum, R.O. (2005). Courting bird sings with stridulating wing feathers. Science *309*, 736. https://doi.org/10.1126/science.1111701.

14. Barske, J., Eghbali, M., Kosarussavadi, S., Choi, E., and Schlinger, B.A. (2019). The heart of an acrobatic bird. Comp. Biochem. Physiol. A Mol. Integr. Physiol. *228*, 9–17. https://doi.org/10.1016/j.cbpa.2018.10.010.

15. Chapman, F.M. (1935). The courtship of Gould's manakin (Manacus vitellinus vitellinus) on Barro Colorado Island, Canal Zone. Bull. AMNH *68*, 7.

16. Ryder, T.B., Parker, P.G., Blake, J.G., and Loiselle, B.A. (2009). It takes two to tango: reproductive skew and social correlates of male mating success in a lek-breeding bird. Proc. Biol. Sci. *276*, 2377–2384. https://doi.org/10.1098/rspb.2009.0208.

17. DuVal, E.H., and Kempenaers, B. (2008). Sexual selection in a lekking bird: the relative opportunity for selection by female choice and male competition. Proc. Biol. Sci. *275*, 1995–2003. https://doi.org/10.1098/rspb.2008.0151.

18. Snow, D.W. (1971). Evolutionary aspects of fruit-eating by birds. Ibis *113*, 194–202. https://doi.org/10.1111/j.1474-919x.1971.tb05144.x.

19. Anderson, H.L., Cabo, J., and Karubian, J. (2024). Fruit resources shape sexual selection processes in a lek mating system. Biol. Lett. *20*, 20240284. https://doi.org/10.1098/rsbl.2024.0284.

20. Théry, M. (1992). The evolution of leks through female choice: differential clustering and space utilization in six sympatric manakins. Behav. Ecol. Sociobiol. *30*, 227–237. https://doi.org/10.1007/BF00166707.

21. Ryder, T.B., Blake, J.G., and Loiselle, B.A. (2006). A test of the environmental hotspot hypothesis for lek placement in three species of manakins (Pipridae) in Ecuador. Auk *123*, 247–258. https://doi.org/10.1093/auk/123.1.247.

22. Loiselle, B.A., Blake, J.G., Durães, R., Ryder, T.B., and Tori, W. (2007). Environmental and spatial segregation of leks among six co-occurring species of manakins (Pipridae) in eastern Ecuador. Auk *124*, 420–431. https://doi.org/10.1093/auk/124.2.420.

23. Barber, R.A., Yang, J., Yang, C., Barker, O., Janicke, T., and Tobias, J.A. (2024). Climate and ecology predict latitudinal trends in sexual selection inferred from avian mating systems. PLOS Biol. *22*, e3002856. https://doi.org/10.1371/journal.pbio.3002856.

24. Amster, G., Murphy, D.A., Milligan, W.R., and Sella, G. (2020). Changes in life history and population size can explain the relative neutral diversity levels on X and autosomes in extant human populations. Proc. Natl. Acad. Sci. USA *117*, 20063–20069. https://doi.org/10.1073/pnas.1915664117.

25. Amster, G., and Sella, G. (2020). Life history effects on neutral diversity levels of autosomes and sex chromosomes. Genetics *215*, 1133–1142. https://doi.org/10.1534/genetics.120.303119.

26. Wilson Sayres, M.A. (2018). Genetic diversity on the sex chromosomes. Genome Biol. Evol. *10*, 1064–1078. https://doi.org/10.1093/gbe/evy039.

27. Corl, A., and Ellegren, H. (2012). The genomic signature of sexual selection in the genetic diversity of the sex chromosomes and autosomes. Evolution *66*, 2138–2149. https://doi.org/10.1111/j.1558-5646.2012.01586.x.

28. Huang, H., and Rabosky, D.L. (2015). Sex-linked genomic variation and its relationship to avian plumage dichromatism and sexual selection. BMC Evol. Biol. *15*, 199. https://doi.org/10.1186/s12862-015-0480-4.

29. Schaedler, L.M., Taylor, L.U., Prum, R.O., and Anciães, M. (2021). Constraint and function in the predefinitive plumages of manakins (Aves: Pipridae). Integr. Comp. Biol. *61*, 1363–1377. https://doi.org/10.1093/icb/icab063.

30. Ryder, T.B., and Sillett, T.S. (2016). Climate, demography and lek stability in an Amazonian bird. Proc. Biol. Sci. *283*, 20152314. https://doi.org/10.1098/rspb.2015.2314.

31. Smith, M.D., Wertheim, J.O., Weaver, S., Murrell, B., Scheffler, K., and Kosakovsky Pond, S.L. (2015). Less is more: an adaptive branch-site random effects model for efficient detection of episodic diversifying selection. Mol. Biol. Evol. *32*, 1342–1353. https://doi.org/10.1093/molbev/msv022.

32. McDonald, J.H., and Kreitman, M. (1991). Adaptive protein evolution at the Adh locus in Drosophila. Nature *351*, 652–654. https://doi.org/10.1038/351652a0.

33. Lim, H.C., Bennett, K.F.P., Justyn, N.M., Powers, M.J., Long, K.M., Kingston, S.E., Lindsay, W.R., Pease, J.B., Fuxjager, M.J., Bolton, P.E., et al. (2024). Sequential introgression of a carotenoid processing gene underlies sexual ornament diversity in a genus of manakins. Sci. Adv. *10*, eadn8339. https://doi.org/10.1126/sciadv.adn8339.

34. Schlinger, B.A., Barske, J., Day, L., Fusani, L., and Fuxjager, M.J. (2013). Hormones and the neuromuscular control of courtship in the golden-collared manakin (Manacus vitellinus). Front. Neuroendocrinol. *34*, 143–156. https://doi.org/10.1016/j.yfrne.2013.04.001.

35. Dennis, G., Jr., Sherman, B.T., Hosack, D.A., Yang, J., Gao, W., Lane, H.C., and Lempicki, R.A. (2003). DAVID: Database for annotation, visualization, and integrated discovery. Genome Biol. *4*, P3. https://doi.org/10.1186/gb-2003-4-9-r60.

36. Huang, D.W., Sherman, B.T., and Lempicki, R.A. (2009). Systematic and integrative analysis of large gene lists using DAVID bioinformatics resources. Nat. Protoc. *4*, 44–57. https://doi.org/10.1038/nprot.2008.211.

37. Lessner, K.M., Dearing, M.D., Izhaki, I., Samuni-Blank, M., Arad, Z., and Karasov, W.H. (2015). Small intestinal hydrolysis of plant glucosides: higher glucohydrolase activities in rodents than passerine birds. J. Exp. Biol. *218*, 2666–2669. https://doi.org/10.1242/jeb.121970.

38. Day, A.J., Cañada, F.J., Díaz, J.C., Kroon, P.A., Mclauchlan, R., Faulds, C.B., Plumb, G.W., Morgan, M.R., and Williamson, G. (2000). Dietary flavonoid and isoflavone glycosides are hydrolysed by the lactase site of lactase phlorizin hydrolase. FEBS Lett. *468*, 166–170. https://doi.org/10.1016/s0014-5793(00)01211-4.

39. Tishkoff, S.A., Reed, F.A., Ranciaro, A., Voight, B.F., Babbitt, C.C., Silverman, J.S., Powell, K., Mortensen, H.M., Hirbo, J.B., Osman, M., et al. (2007). Convergent adaptation of human lactase persistence in Africa and Europe. Nat. Genet. *39*, 31–40. https://doi.org/10.1038/ng1946.

40. Pollock, H.S., Tarwater, C.E., Karr, J.R., and Brawn, J.D. (2024). Long-term monitoring reveals the long lifespans of Neotropical forest landbirds. Ecology *105*, e4386. https://doi.org/10.1002/ecy.4386.

41. Cárdenas-Posada, G., Cadena, C.D., Blake, J.G., and Loiselle, B.A. (2018). Display behaviour, social organization and vocal repertoire of Blue-backed Manakin Chiroxiphia pareola napensis in northwest Amazonia. Ibis *160*, 269–282. https://doi.org/10.1111/ibi.12548.

42. Vernasco, B.J., Dakin, R., Majer, A.D., Haussmann, M.F., Brandt Ryder, T., and Moore, I.T. (2021). Longitudinal dynamics and behavioural correlates of telomeres in male wire-tailed manakins. Funct. Ecol. *35*, 450–462. https://doi.org/10.1111/1365-2435.13715.

43. Stein, A.C., and Uy, J.A.C. (2006). Plumage brightness predicts male mating success in the lekking golden-collared manakin, Manacus vitellinus. Behav. Ecol. *17*, 41–47. https://doi.org/10.1093/beheco/ari095.

44. Day, L.B., Fusani, L., Kim, C., and Schlinger, B.A. (2011). Sexually dimorphic neural phenotypes in golden-collared manakins (Manacus

vitellinus). Brain Behav. Evol. *77*, 206–218. https://doi.org/10.1159/000327046.

45. Fuxjager, M.J., Goller, F., Dirkse, A., Sanin, G.D., and Garcia, S. (2016). Select forelimb muscles have evolved superfast contractile speed to support acrobatic social displays. eLife *5*, e13544. https://doi.org/10.7554/eLife.13544.
46. Agoston, Z., and Schulte, D. (2009). Meis2 competes with the Groucho co-repressor Tle4 for binding to Otx2 and specifies tectal fate without induction of a secondary midbrain-hindbrain boundary organizer. Development *136*, 3311–3322. https://doi.org/10.1242/dev.037770.
47. Bosch, D.G.M., Boonstra, F.N., Gonzaga-Jauregui, C., Xu, M., de Ligt, J., Jhangiani, S., Wiszniewski, W., Muzny, D.M., Yntema, H.G., Pfundt, R., et al. (2014). NR2F1 mutations cause optic atrophy with intellectual disability. Am. J. Hum. Genet. *94*, 303–309. https://doi.org/10.1016/j.ajhg.2014.01.002.
48. Felsen, G., and Mainen, Z.F. (2008). Neural substrates of sensory-guided locomotor decisions in the rat superior colliculus. Neuron *60*, 137–148. https://doi.org/10.1016/j.neuron.2008.09.019.
49. Isa, T., Marquez-Legorreta, E., Grillner, S., and Scott, E.K. (2021). The tectum/superior colliculus as the vertebrate solution for spatial sensory integration and action. Curr. Biol. *31*, R741–R762. https://doi.org/10.1016/j.cub.2021.04.001.
50. Baldwin, M.W., Toda, Y., Nakagita, T., O'Connell, M.J., Klasing, K.C., Misaka, T., Edwards, S.V., and Liberles, S.D. (2014). Sensory biology. Evolution of sweet taste perception in hummingbirds by transformation of the ancestral umami receptor. Science *345*, 929–933. https://doi.org/10.1126/science.1255097.
51. Toda, Y., Ko, M.-C., Liang, Q., Miller, E.T., Rico-Guevara, A., Nakagita, T., Sakakibara, A., Uemura, K., Sackton, T., Hayakawa, T., et al. (2021). Early origin of sweet perception in the songbird radiation. Science *373*, 226–231. https://doi.org/10.1126/science.abf6505.
52. Cramer, J.F., Miller, E.T., Ko, M.-C., Liang, Q., Cockburn, G., Nakagita, T., Cardinale, M., Fusani, L., Toda, Y., and Baldwin, M.W. (2022). A single residue confers selective loss of sugar sensing in wrynecks. Curr. Biol. *32*, 4270–4278.e5. https://doi.org/10.1016/j.cub.2022.07.059.
53. Levey, D.J. (1987). Sugar-tasting ability and fruit selection in tropical fruit-eating birds. Auk *104*, 173–179. https://doi.org/10.1093/auk/104.2.173.
54. Pizo, M.A., Morales, J.M., Ovaskainen, O., and Carlo, T.A. (2021). Frugivory specialization in birds and fruit chemistry structure mutualistic networks across the Neotropics. Am. Nat. *197*, 236–249. https://doi.org/10.1086/712381.
55. Cipollini, M.L., and Levey, D.J. (1997). Secondary metabolites of fleshy vertebrate-dispersed fruits: adaptive hypotheses and implications for seed dispersal. Am. Nat. *150*, 346–372. https://doi.org/10.1086/286069.
56. Cestari, C., and Pizo, M.A. (2013). Frugivory by the White-bearded Manakin (Manacus manacus, Pipridae) in restinga forest, an ecosystem associated to the Atlantic forest. Biota Neotrop. *13*, 345–350. https://doi.org/10.1590/s1676-06032013000200038.
57. Levey, D.J., Moermond, T.C., and Denslow, J.S. (1984). Fruit choice in neotropical birds: The effect of distance between fruits on preference patterns. Ecology *65*, 844–850. https://doi.org/10.2307/1938058.
58. Foster, M.S. (1977). Ecological and nutritional effects of food scarcity on a tropical frugivorous bird and its fruit source. Ecology *58*, 73–85. https://doi.org/10.2307/1935109.
59. Struempf, H.G., Schondube, J.E., and Del Rio, C.M. (1999). The cyanogenic glycoside amygdalin does not deter consumption of ripe fruit by cedar waxwings. Auk *116*, 749–758. https://doi.org/10.2307/4089335.
60. Dostanic, I., Schultz, J.E.J., Lorenz, J.N., and Lingrel, J.B. (2004). The alpha 1 isoform of Na,K-ATPase regulates cardiac contractility and functionally interacts and co-localizes with the Na/Ca exchanger in heart. J. Biol. Chem. *279*, 54053–54061. https://doi.org/10.1074/jbc.M410737200.
61. Taverner, A.M., Yang, L., Barile, Z.J., Lin, B., Peng, J., Pinharanda, A.P., Rao, A.S., Roland, B.P., Talsma, A.D., Wei, D., et al. (2019). Adaptive substitutions underlying cardiac glycoside insensitivity in insects exhibit epistasis in vivo. eLife *8*, e48224. https://doi.org/10.7554/eLife.48224.
62. Mohammadi, S., Yang, L., Harpak, A., Herrera-Álvarez, S., Del Pilar Rodríguez-Ordoñez, M., Peng, J., Zhang, K., Storz, J.F., Dobler, S., Crawford, A.J., et al. (2021). Concerted evolution reveals co-adapted amino acid substitutions in Na+K+-ATPase of frogs that prey on toxic toads. Curr. Biol. *31*, 2530–2538.e10. https://doi.org/10.1016/j.cub.2021.03.089.
63. Arribas, J.C., Herrero, A.G., Martín-Lomas, M., Cañada, F.J., He, S., and Withers, S.G. (2000). Differential mechanism-based labeling and unequivocal activity assignment of the two active sites of intestinal lactase/phlorizin hydrolase. Eur. J. Biochem. *267*, 6996–7005. https://doi.org/10.1046/j.1432-1327.2000.01784.x.
64. Siddons, R.C., and Coates, M.E. (1972). The influence of the intestinal microflora on disaccharidase activities in the chick. Br. J. Nutr. *27*, 101–112. https://doi.org/10.1079/bjn19720074.
65. Tewksbury, J.J., and Nabhan, G.P. (2001). Directed deterrence by capsaicin in chillies. Nature *412*, 403–404. https://doi.org/10.1038/35086653.
66. Hasan, F.M., Alsahli, M., and Gerich, J.E. (2014). SGLT2 inhibitors in the treatment of type 2 diabetes. Diabetes Res. Clin. Pract. *104*, 297–322. https://doi.org/10.1016/j.diabres.2014.02.014.
67. Tobias, J.A., Sheard, C., Seddon, N., Meade, A., Cotton, A.J., and Nakagawa, S. (2016). Territoriality, social bonds, and the evolution of communal signaling in birds. Front. Ecol. Evol. *4*. https://doi.org/10.3389/fevo.2016.00074.
68. Dale, J., Dey, C.J., Delhey, K., Kempenaers, B., and Valcu, M. (2015). The effects of life history and sexual selection on male and female plumage colouration. Nature *527*, 367–370. https://doi.org/10.1038/nature15509.
69. Wilman, H., Belmaker, J., Simpson, J., de la Rosa, C., Rivadeneira, M.M., and Jetz, W. (2014). EltonTraits 1.0: Species-level foraging attributes of the world's birds and mammals. Ecology *95*, 2027. https://doi.org/10.1890/13-1917.1.
70. Harvey, M.G., Bravo, G.A., Claramunt, S., Cuervo, A.M., Derryberry, G.E., Battilana, J., Seeholzer, G.F., McKay, J.S., O'Meara, B.C., Faircloth, B.C., et al. (2020). The evolution of a tropical biodiversity hotspot. Science *370*, 1343–1348. https://doi.org/10.1126/science.aaz6970.
71. Beehler, B. (1983). Frugivory and polygamy in birds of paradise. Auk *100*, 1–12. https://doi.org/10.1093/auk/100.1.1.
72. Shogren, E.H.. Dancing in the Rain: Selective Drivers of Variability in Neotropical Manakins. https://hdl.handle.net/2097/40795.
73. Dimitrieva, S., and Bucher, P. (2013). UCNEbase-a database of ultraconserved non-coding elements and genomic regulatory blocks. Nucleic Acids Res. *41*, D101–D109. https://doi.org/10.1093/nar/gks1092.
74. Zimin, A.V., Marçais, G., Puiu, D., Roberts, M., Salzberg, S.L., and Yorke, J.A. (2013). The MaSuRCA genome assembler. Bioinformatics *29*, 2669–2677. https://doi.org/10.1093/bioinformatics/btt476.
75. Luo, R., Liu, B., Xie, Y., Li, Z., Huang, W., Yuan, J., He, G., Chen, Y., Pan, Q., Liu, Y., et al. (2012). SOAPdenovo2: an empirically improved memory-efficient short-read de novo assembler. GigaScience *1*, 18. https://doi.org/10.1186/2047-217X-1-18.
76. Langmead, B., and Salzberg, S.L. (2012). Fast gapped-read alignment with Bowtie 2. Nat. Methods *9*, 357–359. https://doi.org/10.1038/nmeth.1923.
77. Walker, B.J., Abeel, T., Shea, T., Priest, M., Abouelliel, A., Sakthikumar, S., Cuomo, C.A., Zeng, Q., Wortman, J., Young, S.K., et al. (2014). Pilon: an integrated tool for comprehensive microbial variant detection and genome assembly improvement. PLOS One *9*, e112963. https://doi.org/10.1371/journal.pone.0112963.
78. English, A.C., Richards, S., Han, Y., Wang, M., Vee, V., Qu, J., Qin, X., Muzny, D.M., Reid, J.G., Worley, K.C., et al. (2012). Mind the gap: upgrading genomes with Pacific Biosciences RS long-read sequencing

technology. PLOS One *7*, e47768. https://doi.org/10.1371/journal.pone.0047768.

79. Maccallum, I., Przybylski, D., Gnerre, S., Burton, J., Shlyakhter, I., Gnirke, A., Malek, J., McKernan, K., Ranade, S., Shea, T.P., et al. (2009). ALLPATHS 2: small genomes assembled accurately and with high continuity from short paired reads. Genome Biol. *10*, R103. https://doi.org/10.1186/gb-2009-10-10-r103.
80. Tsai, I.J., Otto, T.D., and Berriman, M. (2010). Improving draft assemblies by iterative mapping and assembly of short reads to eliminate gaps. Genome Biol. *11*, R41. https://doi.org/10.1186/gb-2010-11-4-r41.
81. Boetzer, M., Henkel, C.V., Jansen, H.J., Butler, D., and Pirovano, W. (2011). Scaffolding pre-assembled contigs using SSPACE. Bioinformatics *27*, 578–579. https://doi.org/10.1093/bioinformatics/btq683.
82. Armstrong, J., Hickey, G., Diekhans, M., Fiddes, I.T., Novak, A.M., Deran, A., Fang, Q., Xie, D., Feng, S., Stiller, J., et al. (2020). Progressive Cactus is a multiple-genome aligner for the thousand-genome era. Nature *587*, 246–251. https://doi.org/10.1038/s41586-020-2871-y.
83. Smit, A.F.A., Hubley, R., and Green, P. (2013–2015). RepeatMasker Open-4.0. www.repeatmasker.org.
84. Kolmogorov, M., Raney, B., Paten, B., and Pham, S. (2014). Ragout-a reference-assisted assembly tool for bacterial genomes. Bioinformatics *30*, i302–i309. https://doi.org/10.1093/bioinformatics/btu280.
85. Li, H., and Durbin, R. (2010). Fast and accurate long-read alignment with Burrows-Wheeler transform. Bioinformatics *26*, 589–595. https://doi.org/10.1093/bioinformatics/btp698.
86. Li, H. (2011). A statistical framework for SNP calling, mutation discovery, association mapping and population genetical parameter estimation from sequencing data. Bioinformatics *27*, 2987–2993. https://doi.org/10.1093/bioinformatics/btr509.
87. Danecek, P., Auton, A., Abecasis, G., Albers, C.A., Banks, E., DePristo, M.A., Handsaker, R.E., Lunter, G., Marth, G.T., Sherry, S.T., et al. (2011). The variant call format and VCFtools. Bioinformatics *27*, 2156–2158. https://doi.org/10.1093/bioinformatics/btr330.
88. Korunes, K.L., and Samuk, K. (2021). pixy: Unbiased estimation of nucleotide diversity and divergence in the presence of missing data. Mol. Ecol. Resour. *21*, 1359–1368. https://doi.org/10.1111/1755-0998.13326.
89. Alonge, M., Lebeigle, L., Kirsche, M., Jenike, K., Ou, S., Aganezov, S., Wang, X., Lippman, Z.B., Schatz, M.C., and Soyk, S. (2022). Automated assembly scaffolding using RagTag elevates a new tomato system for high-throughput genome editing. Genome Biol. *23*, 258. https://doi.org/10.1186/s13059-022-02823-7.
90. DePristo, M.A., Banks, E., Poplin, R., Garimella, K.V., Maguire, J.R., Hartl, C., Philippakis, A.A., del Angel, G., Rivas, M.A., Hanna, M., et al. (2011). A framework for variation discovery and genotyping using next-generation DNA sequencing data. Nat. Genet. *43*, 491–498. https://doi.org/10.1038/ng.806.
91. Cingolani, P., Platts, A., Wang, L.L., Coon, M., Nguyen, T., Wang, L., Land, S.J., Lu, X., and Ruden, D.M. (2012). A program for annotating and predicting the effects of single nucleotide polymorphisms, SnpEff: SNPs in the genome of Drosophila melanogaster strain w1118; iso-2; iso-3. Fly (Austin) *6*, 80–92. https://doi.org/10.4161/fly.19695.
92. R Core Team (2021). R: a Language and Environment for Statistical Computing (R Foundation for Statistical Computing).
93. Katoh, K., Kuma, K.-I., Toh, H., and Miyata, T. (2005). MAFFT version 5: improvement in accuracy of multiple sequence alignment. Nucleic Acids Res. *33*, 511–518. https://doi.org/10.1093/nar/gki198.
94. Suyama, M., Torrents, D., and Bork, P. (2006). PAL2NAL: robust conversion of protein sequence alignments into the corresponding codon alignments. Nucleic Acids Res. *34*, W609–W612. https://doi.org/10.1093/nar/gkl315.
95. Misof, B., and Misof, K. (2009). A Monte Carlo Approach Successfully Identifies Randomness in Multiple Sequence Alignments: A More Objective Means of Data Exclusion. Syst. Biol. *58*, 21–34. https://doi.org/10.1093/sysbio/syp006.
96. Kück, P., Meusemann, K., Dambach, J., Thormann, B., von Reumont, B.M., Wägele, J.W., and Misof, B. (2010). Parametric and non-parametric masking of randomness in sequence alignments can be improved and leads to better resolved trees. Front. Zool. *7*, 10. https://doi.org/10.1186/1742-9994-7-10.
97. Harrison, P.W., Jordan, G.E., and Montgomery, S.H. (2014). SWAMP: Sliding Window Alignment Masker for PAML. Evol. Bioinform. Online *10*, 197–204. https://doi.org/10.4137/EBO.S18193.
98. Altschul, S.F., Gish, W., Miller, W., Myers, E.W., and Lipman, D.J. (1990). Basic local alignment search tool. J. Mol. Biol. *215*, 403–410. https://doi.org/10.1016/S0022-2836(05)80360-2.
99. Freedman, A.H., Clamp, M., and Sackton, T.B. (2021). Error, noise and bias in de novo transcriptome assemblies. Mol. Ecol. Resour. *21*, 18–29. https://doi.org/10.1111/1755-0998.13156.
100. Andrews, S. (2010). FastQC: A Quality Control Tool for High Throughput Sequence Data. http://www.bioinformatics.babraham.ac.uk/projects/fastqc.
101. Song, L., and Florea, L. (2015). Rcorrector: efficient and accurate error correction for Illumina RNA-seq reads. GigaScience *4*, 48. https://doi.org/10.1186/s13742-015-0089-y.
102. Dobin, A., Davis, C.A., Schlesinger, F., Drenkow, J., Zaleski, C., Jha, S., Batut, P., Chaisson, M., and Gingeras, T.R. (2013). STAR: ultrafast universal RNA-seq aligner. Bioinformatics *29*, 15–21. https://doi.org/10.1093/bioinformatics/bts635.
103. Pennell, M.W., Eastman, J.M., Slater, G.J., Brown, J.W., Uyeda, J.C., FitzJohn, R.G., Alfaro, M.E., and Harmon, L.J. (2014). Geiger v2.0: An expanded suite of methods for fitting macroevolutionary models to phylogenetic trees. Bioinformatics *30*, 2216–2218. https://doi.org/10.1093/bioinformatics/btu181.
104. Edgar, R.C. (2022). Muscle5: High-accuracy alignment ensembles enable unbiased assessments of sequence homology and phylogeny. Nat. Commun. *13*, 6968. https://doi.org/10.1038/s41467-022-34630-w.
105. Schliep, K.P. (2011). phangorn: phylogenetic analysis in R. Bioinformatics *27*, 592–593. https://doi.org/10.1093/bioinformatics/btq706.
106. Paradis, E., and Schliep, K. (2019). ape 5.0: an environment for modern phylogenetics and evolutionary analyses in R. Bioinformatics *35*, 526–528. https://doi.org/10.1093/bioinformatics/bty633.
107. Ashkenazy, H., Penn, O., Doron-Faigenboim, A., Cohen, O., Cannarozzi, G., Zomer, O., and Pupko, T. (2012). FastML: a web server for probabilistic reconstruction of ancestral sequences. Nucleic Acids Res. *40*, W580–W584. https://doi.org/10.1093/nar/gks498.
108. Abascal, F., Zardoya, R., and Telford, M.J. (2010). TranslatorX: multiple alignment of nucleotide sequences guided by amino acid translations. Nucleic Acids Res. *38*, W7–W13. https://doi.org/10.1093/nar/gkq291.
109. Weaver, S., Shank, S.D., Spielman, S.J., Li, M., Muse, S.V., and Kosakovsky Pond, S.L. (2018). Datamonkey 2.0: A modern web application for characterizing selective and other evolutionary processes. Mol. Biol. Evol. *35*, 773–777. https://doi.org/10.1093/molbev/msx335.
110. Wertheim, J.O., Murrell, B., Smith, M.D., Kosakovsky Pond, S.L., and Scheffler, K. (2015). RELAX: detecting relaxed selection in a phylogenetic framework. Mol. Biol. Evol. *32*, 820–832. https://doi.org/10.1093/molbev/msu400.
111. Castresana, J. (2000). Selection of conserved blocks from multiple alignments for their use in phylogenetic analysis. Mol. Biol. Evol. *17*, 540–552. https://doi.org/10.1093/oxfordjournals.molbev.a026334.
112. Lawrence, M., Huber, W., Pagès, H., Aboyoun, P., Carlson, M., Gentleman, R., Morgan, M.T., and Carey, V.J. (2013). Software for computing and annotating genomic ranges. PLOS Comput. Biol. *9*, e1003118. https://doi.org/10.1371/journal.pcbi.1003118.
113. Chen, Y., Chen, L., Lun, A.T.L., Baldoni, P.L., and Smyth, G.K. (2025). edgeR v4: powerful differential analysis of sequencing data with expanded functionality and improved support for small counts and larger

datasets. Nucleic Acids Res. *53*, gkaf018. https://doi.org/10.1093/nar/gkaf018.

114. Revell, L.J. (2012). phytools: an R package for phylogenetic comparative biology (and other things). Methods Ecol. Evol. *3*, 217–223. https://doi.org/10.1111/j.2041-210x.2011.00169.x.
115. Beaulieu, J.M., O'Meara, B.C., and Donoghue, M.J. (2013). Identifying hidden rate changes in the evolution of a binary morphological character: the evolution of plant habit in campanulid angiosperms. Syst. Biol. *62*, 725–737. https://doi.org/10.1093/sysbio/syt034.
116. Miller, E.T., and Martin, B.S. (2022). Distilling complex evolutionary histories with shiftPlot. Preprint at bioRxiv. https://doi.org/10.1101/2022.03.16.484646.
117. Bastide, P., Ané, C., Robin, S., and Mariadassou, M. (2018). Inference of adaptive shifts for multivariate correlated traits. Syst. Biol. *67*, 662–680. https://doi.org/10.1093/sysbio/syy005.
118. Bastide, P., Mariadassou, M., and Robin, S. (2017). Detection of adaptive shifts on phylogenies by using shifted stochastic processes on a tree. J. R. Stat. Soc. B *79*, 1067–1093. https://doi.org/10.1111/rssb.12206.
119. Horton, B.M., Ryder, T.B., Moore, I.T., and Balakrishnan, C.N. (2020). Gene expression in the social behavior network of the wire-tailed manakin (Pipra filicauda) brain. Genes Brain Behav. *19*, e12560. https://doi.org/10.1111/gbb.12560.
120. Del-Rio, G., Rego, M.A., Whitney, B.M., Schunck, F., Silveira, L.F., Faircloth, B.C., and Brumfield, R.T. (2022). Displaced clines in an avian hybrid zone (Thamnophilidae: Rhegmatorhina) within an Amazonian interfluve. Evolution *76*, 455–475. https://doi.org/10.1111/evo.14377.
121. Bemmels, J.B., Bramwell, A.C., Anderson, S.A.S., Luzuriaga-Aveiga, V.E., Mikkelsen, E.K., and Weir, J.T. (2021). Geographic contact drives increased reproductive isolation in two cryptic Empidonax flycatchers. Mol. Ecol. *30*, 4833–4844. https://doi.org/10.1111/mec.16105.
122. Long, K.M., Rivera-Colón, A.G., Bennett, K.F.P., Catchen, J.M., Braun, M.J., and Brawn, J.D. (2024). Ongoing introgression of a secondary sexual plumage trait in a stable avian hybrid zone. Evolution *78*, 1539–1553. https://doi.org/10.1093/evolut/qpae076.
123. Barrera-Guzmán, A.O., Aleixo, A., Faccio, M., Dantas, S. de M., and Weir, J.T. (2022). Gene flow, genomic homogenization and the timeline to speciation in Amazonian manakins. Mol. Ecol. *31*, 4050–4066. https://doi.org/10.1111/mec.16562.
124. Moncrieff, A.E., Faircloth, B.C., and Brumfield, R.T. (2022). Systematics of Lepidothrix manakins (Aves: Passeriformes: Pipridae) using RADcap markers. Mol. Phylogenet. Evol. *173*, 107525. https://doi.org/10.1016/j.ympev.2022.107525.
125. Jarvis, E.D., Mirarab, S., Aberer, A.J., Li, B., Houde, P., Li, C., Ho, S.Y.W., Faircloth, B.C., Nabholz, B., Howard, J.T., et al. (2014). Whole-genome analyses resolve early branches in the tree of life of modern birds. Science *346*, 1320–1331. https://doi.org/10.1126/science.1253451.
126. Bostwick, K.S., and Prum, R.O. (2003). High-speed video analysis of wing-snapping in two manakin clades(Pipridae: Aves). J. Exp. Biol. *206*, 3693–3706. https://doi.org/10.1242/jeb.00598.
127. Barske, J., Schlinger, B.A., and Fusani, L. (2015). The presence of a female influences courtship performance of male manakins. Auk *132*, 594–603. https://doi.org/10.1642/auk-14-92.1.
128. Hahn, M.W. (2018). Molecular Population Genetics (Oxford University Press Academic).
129. National Center for Biotechnology Information NCBI Software Development Toolkit.
130. Sackton, T.B., Lazzaro, B.P., Schlenke, T.A., Evans, J.D., Hultmark, D., and Clark, A.G. (2007). Dynamic evolution of the innate immune system in Drosophila. Nat. Genet. *39*, 1461–1468. https://doi.org/10.1038/ng.2007.60.
131. Casagrande, S., and Hau, M. (2019). Telomere attrition: metabolic regulation and signalling function? Biol. Lett. *15*, 20180885. https://doi.org/10.1098/rsbl.2018.0885.
132. Feng, S., Stiller, J., Deng, Y., Armstrong, J., Fang, Q., Reeve, A.H., Xie, D., Chen, G., Guo, C., Faircloth, B.C., et al. (2020). Dense sampling of bird diversity increases power of comparative genomics. Nature *587*, 252–257. https://doi.org/10.1038/s41586-020-2873-9.
133. Ruegg, K., Bay, R.A., Anderson, E.C., Saracco, J.F., Harrigan, R.J., Whitfield, M., Paxton, E.H., and Smith, T.B. (2018). Ecological genomics predicts climate vulnerability in an endangered southwestern songbird. Ecol. Lett. *21*, 1085–1096. https://doi.org/10.1111/ele.12977.
134. Warren, W.C., Clayton, D.F., Ellegren, H., Arnold, A.P., Hillier, L.W., Künstner, A., Searle, S., White, S., Vilella, A.J., Fairley, S., et al. (2010). The genome of a songbird. Nature *464*, 757–762. https://doi.org/10.1038/nature08819.
135. Wirthlin, M., Lima, N.C.B., Guedes, R.L.M., Soares, A.E.R., Almeida, L.G.P., Cavaleiro, N.P., Loss de Morais, G., Chaves, A.V., Howard, J.T., Teixeira, M. de M., et al. (2018). Parrot genomes and the evolution of heightened longevity and cognition. Curr. Biol. *28*, 4001–4008.e7. https://doi.org/10.1016/j.cub.2018.10.050.
136. Zhang, G., Li, C., Li, Q., Li, B., Larkin, D.M., Lee, C., Storz, J.F., Antunes, A., Greenwold, M.J., Meredith, R.W., et al. (2014). Comparative genomics reveals insights into avian genome evolution and adaptation. Science *346*, 1311–1320. https://doi.org/10.1126/science.1251385.
137. Lovell, P.V., Wirthlin, M., Kaser, T., Buckner, A.A., Carleton, J.B., Snider, B.R., McHugh, A.K., Tolpygo, A., Mitra, P.P., and Mello, C.V. (2020). ZEBrA: zebra finch Expression Brain Atlas-A resource for comparative molecular neuroanatomy and brain evolution studies. J. Comp. Neurol. *528*, 2099–2131. https://doi.org/10.1002/cne.24879.
138. Cockburn, G., Ko, M.-C., Sadanandan, K.R., Miller, E.T., Nakagita, T., Monte, A., Cho, S., Roura, E., Toda, Y., and Baldwin, M.W. (2022). Synergism, Bifunctionality, and the Evolution of a Gradual Sensory Trade-off in Hummingbird Taste Receptors. Mol. Biol. Evol. *39*, msab367. https://doi.org/10.1093/molbev/msab367.
139. Brun, A., Mendez-Aranda, D., Magallanes, M.E., Karasov, W.H., Martínez Del Rio, C., Baldwin, M.W., and Caviedes-Vidal, E. (2020). Duplications and functional convergence of intestinal carbohydrate-digesting enzymes. Mol. Biol. Evol. *37*, 1657–1666. https://doi.org/10.1093/molbev/msaa034.
140. Tribble, C.M., May, M.R., Jackson-Gain, A., Zenil-Ferguson, R., Specht, C.D., and Rothfels, C.J. (2023). Unearthing modes of climatic adaptation in underground storage organs across Liliales. Syst. Biol. *72*, 198–212. https://doi.org/10.1093/sysbio/syac070.

Please cite this article in press as: Balakrishnan et al., Genomic and physiological changes in a sexually selected and frugivorous bird radiation, Current Biology (2026), https://doi.org/10.1016/j.cub.2026.05.021





## STAR★METHODS

### KEY RESOURCES TABLE

| REAGENT or RESOURCE | SOURCE | IDENTIFIER |
|---|---|---|
| Antibodies | | |
| Alkaline phosphatase-conjugated anti-DIG antibody | Roche | Cat#11093274910; RRID: AB_2313640 |
| Biological samples | | |
| *Lepidothrix coronata* muscle tissue for genome | Louisiana State University, Museum of Zoology | LSUMZ B3197, #110521 |
| *Pipra filicauda* muscle tissue for genome | Louisiana State University, Museum of Zoology | LSUMZ B4331, #115617 |
| *Neopelma chrysocephalum* muscle tissue for genome | Yale Peabody Museum, Vertebrate Zoology, Division Ornithology | YPM-ORN-139661 |
| *Neopelma chrysocephalum* tissue for RADseq (*n*=7) | Smithsonian National Museum of Natural History | 627212, 627076, 659093, 659094, 625577, 625578, and 625576 |
| *Manacus vitellinus* tissue for genome | This paper | BGI_N305 |
| *Corapipo altera* liver and musle tissues for genome | This paper | COAL_440 |
| *Manacus vitellinus* tissues for RNA-seq (kidney, brain, liver) | This paper | PRJNA320632 |
| *Lepidothrix coronata* tissues for RNA-seq (liver, testis, muscle) | This paper | PRJNA321179 |
| *Manacus vitellinus* liver tissue | This paper | MV-58-LV |
| *Manacus vitellinus* kidney tissue | This paper | MV-58-KD |
| *Manacus vitellinus* digestive tract tissue | This paper | MV-58-DT |
| *Manacus vitellinus* liver tissue | This paper | MV-57-LV |
| *Manacus vitellinus* kidney tissue | This paper | MV-57-KD |
| *Manacus vitellinus* digestive tract tissue | This paper | MV-57-DT |
| *Manacus vitellinus* liver tissue | This paper | MV-40-LV |
| *Manacus vitellinus* kidney tissue | This paper | MV-40-KD |
| *Manacus vitellinus* digestive tract tissue | This paper | MV-40-LV |
| *Corapipo altera* blood samples (*n*=33) | Shogren[72] (thesis) | N/A |
| *Manacus candei* genomic DNA derived from specimens (*n*=22) | Smithsonian National Museum of Natural History | B04590, B01878, B01883, B01884, B01886, B01888, B01890, B01891, B01894, B01921, B01922, B01924, B01897, B01898, B01899, B01903, B01908, B01909, B01910, B01911, B01948, B01949 |
| *Neopelma chrysocephalum* tissue for *T1R* amplification | Louisiana State University, Museum of Zoology | LSUMZ B25410 |
| *Lepidothrix coronata* tissue for *T1R* amplification | Louisiana State University, Museum of Zoology | LSUMZ B3197 |
| Zebra finch (*Taeniopygia guttata*) brain tissue sections | Mello lab collection | N/A |
| *Ceratopipra rubrocapilla* brain sections | Museu Paraense Emilio Goeldi | N/A |
| Chemicals, peptides, and recombinant proteins | | |
| T3 RNA polymerase | Promega | Cat# 2083 |
| DIG RNA labeling mix | Roche | Cat# 11277073910 |
| BCIP/NBT Substrate Solution | PerkinElmer | Cat# NEL937001PK |
| VectaMount permanent mounting medium | Vector Laboratories | Cat# H-5600-60 |
| Lactose | Carl Roth | Cat# 6868.1 |
| Phlorizin | Sigma Aldrich | Cat# CDS000104 |

(*Continued on next page*)

Please cite this article in press as: Balakrishnan et al., Genomic and physiological changes in a sexually selected and frugivorous bird radiation, Current Biology (2026), https://doi.org/10.1016/j.cub.2026.05.021



***Continued***

| REAGENT or RESOURCE | SOURCE | IDENTIFIER |
|---|---|---|
| Critical commercial assays | | |
| NEBNext Ultra II RNA Library Preparation Kit | New England Biolabs (NEB) | Cat# E7770 |
| QIAprep Spin Miniprep Kit | QIAGEN | Cat# 27104 |
| QIAquick PCR purification kit | QIAGEN | Cat# 28104 |
| DNeasy Blood & Tissue Kit | Qiagen | Cat# 69504 |
| Sucrose Assay Kit | Abcam | Cat# ab83387 |
| Deposited data | | |
| *Lepidothrix coronata* genome assembly | This paper | GCA_001604755.1 |
| *Pipra filicauda* genome assembly | This paper | GCA_003945595.2 |
| *Neopelma chrysocephalum* genome assembly | This paper | GCA_003984885.2 |
| *Manacus vitellinus* genome assembly | This paper | GCA_001715985.3 (ASM171598v3) |
| *Corapipo altera* genome assembly | This paper | GCA_003945725.1 |
| *Manacus vitellinus* transcriptome | This paper | SRR3476292 |
| *Myiozetetes cayanensis* reference genome assembly (mined for *LPH* prediction) | NCBI RefSeq | GCF_022539395.1 |
| *Lepidothrix coronata* transcriptome | This paper | SRR3493972 |
| *Pipra filicauda* brain transcriptome | NCBI SRA | SRS3023389 |
| *Pipra filicauda* testes transcriptome | NCBI SRA | SRS3023390 |
| *Pipra filicauda* brain transcriptome | NCBI SRA | SRS3023391 |
| *Pipra filicauda* brain transcriptome | NCBI SRA | SRS3023392 |
| *Pipra filicauda* brain transcriptome | NCBI SRA | SRS3023393 |
| *Pipra filicauda* brain transcriptome | NCBI SRA | SRS3023394 |
| *Manacus vitellinus* liver transcriptome | This paper | SRR22012352 |
| *Manacus vitellinus* kidney transcriptome | This paper | SRR22012353 |
| *Manacus vitellinus* digestive tract transcriptome | This paper | SRR22012354 |
| *Manacus vitellinus* liver transcriptome | This paper | SRR22012355 |
| *Manacus vitellinus* kidney transcriptome | This paper | SRR22012356 |
| *Manacus vitellinus* digestive tract transcriptome | This paper | SRR22012357 |
| *Manacus vitellinus* liver transcriptome | This paper | SRR22012359 |
| *Manacus vitellinus* kidney transcriptome | This paper | SRR22012358 |
| *Manacus vitellinus* digestive tract transcriptome | This paper | SRR22012360 |
| *Rhegmatorhina berlepschi* RADseq population samples (*n*=11) | NCBI SRA | PRJNA763942; samples: SRR35754672, SRR35754673, SRR35754695, SRR35754696, SRR35754717, SRR35754738, SRR35754748, SRR35754760, SRR35754777, SRR3575480, SRR35754834 |
| *Empidonax alnorum* RADseq population samples (*n*=13) | NCBI SRA | PRJNA692615; samples: SRR14848188, SRR14848190, SRR14848302, SRR14848303, SRR14848310, SRR14848313, SRR14848314, SRR14848315, SRR14848318, SRR14848320, SRR14848321, SRR14848322, SRR14848333 |

(*Continued on next page*)

Please cite this article in press as: Balakrishnan et al., Genomic and physiological changes in a sexually selected and frugivorous bird radiation, Current Biology (2026), https://doi.org/10.1016/j.cub.2026.05.021





*Continued*

| REAGENT or RESOURCE | SOURCE | IDENTIFIER |
|---|---|---|
| *Manacus vitellinus* RADseq population samples (*n*=20) | NCBI SRA | PRJNA893627; samples: SRR22133426, SRR22133437, SRR22133438, SRR22134030, SRR22134035, SRR22134037, SRR22134038, SRR22134058, SRR22134059, SRR22134070, SRR22134093, SRR22143061, SRR22143084, SRR22143106, SRR22143115, SRR22143117, SRR22143121, SRR22143124, SRR22158168, SRR22158173 |
| *Pipra filicauda* RADseq population samples (*n*=2) | NCBI SRA | PRJNA837991; samples SRR19417635 and SRR19417717 |
| *Lepidothrix coronata* RADseq population samples (*n*=6) | NCBI SRA | PRJNA787238; samples SRR17237521, SRR17237542, SRR17237543, SRR17237574, SRR17237576, SRR17237584 |
| *Corapipo altera* RADseq blood samples (*n*=33) | Shogren[72] (thesis) | SRA submission in progress |
| *Neopelma chrysocephalum* RADseq samples (*n*=7) | This paper | SRA submission in progress |
| *Manacus candei* whole genome resequencing (*n*=22) | Lim et al.[33] | PRJNA1129471; samples SRR29638655, SRR29638669, SRR29638671, SRR29638673, SRR29638676, SRR29638677, SRR29638678, SRR29638679, SRR29638680, SRR29638650, SRR29638651, SRR29638652, SRR29638653, SRR29638654, SRR29638661, SRR29638667, SRR29638668, SRR29638670, SRR29638674, SRR29638675, SRR29638681, SRR29638682 |
| *Lepidothrix coronata* NCBI genome annotation | NCBI RefSeq | https://www.ncbi.nlm.nih.gov/refseq/annotation_euk/Lepidothrix_coronata/100/ |
| *Pipra filicauda* NCBI genome annotation | NCBI RefSeq | https://www.ncbi.nlm.nih.gov/refseq/annotation_euk/Pipra_filicauda/101/ |
| *Manacus vitellinus* NCBI genome annotation | NCBI RefSeq | https://www.ncbi.nlm.nih.gov/refseq/annotation_euk/Manacus_vitellinus/103/ |
| *Taeniopygia guttata* genome assembly | NCBI GenBank | GCA_003957565.4 |
| *Chiroxiphia lanceolata* genome assembly | NCBI RefSeq | GCF_009829145.1 (bChiLan1.pri) |
| *Manacus vitellinus* reference genome assembly | NCBI RefSeq | GCF_001715985.3 |
| *Rhegmatorhina hoffmannsi* reference genome assembly | NCBI RefSeq | LSU_RhHo_2.0 |
| *Empidonax traillii* genome assembly | NCBI RefSeq | ASM303162v1 |
| *Pipra filicauda* whole genome sequencing reads | NCBI SRA | SRR6885520 |
| *Ficedula albicollis* gene predictions | NCBI RefSeq | GCF_000247815.1_FicAlb1.5 |
| *Corvus cornix* gene predictions | NCBI RefSeq | GCF_000738735.2_ASM73873v2 |
| *Empidonax traillii* gene predictions | NCBI RefSeq | GCF_003031625.1_ASM303162v1 |
| *Aquila chrysaetos* gene predictions | NCBI RefSeq | GCF_900496995.1_bAquChr1.2 |
| *Melopsittacus undulatus* gene predictions | NCBI RefSeq | GCF_000238935.1_Melopsittacus_undulatus_6.3 |
| SILVA rRNA dataset, the SSU Parc and LSU Parc sets, release 132 | silva | https://www.arb-silva.de/ |
| UCNEbase | Dimitrieva and Bucher[73] | https://epd.expasy.org/ucnebase/ |
| Neotropical frugivory visits dataset | Pizo et al.[54] | https://github.com/jmmorales/lipids/tree/v01/data |
| Active form of mGluR5 | Protein Data Bank | PDB: 6N51 |

(*Continued on next page*)

Please cite this article in press as: Balakrishnan et al., Genomic and physiological changes in a sexually selected and frugivorous bird radiation, Current Biology (2026), https://doi.org/10.1016/j.cub.2026.05.021



**Continued**

| REAGENT or RESOURCE | SOURCE | IDENTIFIER |
|---|---|---|
| *Neopelma chrysocephalum T1R1* complete coding sequence | This paper | Zenodo:18416735 |
| *Neopelma chrysocephalum T1R3* complete coding sequence | This paper | Zenodo: 18416735 |
| *Lepidothrix coronata T1R1* complete coding sequence | This paper | Zenodo: 18416735 |
| *Lepidothrix coronata T1R3* complete coding sequence | This paper | Zenodo: 18416735 |
| Ancestral reconstructions of T1Rs and LPH | This paper | Zenodo: 18416735 |
| **Experimental models: Cell lines** | | |
| HEK293T | DSMZ-Leibniz Institute | #ACC 635 |
| HEK293T | Matsunami laboratory, Duke University, USA | N/A |
| **Experimental models: Organisms/strains** | | |
| *Neopelma chrysocephalum* for genome | This paper | YPM-ORN-139661 |
| *Corapipo altera* for genome | This paper | COAL_440 |
| *Pipra filicauda* for genome | This paper | LSUMZ B4331 #115617 |
| *Lepidothrix coronata* for genome | This paper | LSUMZ B3197 #110521 |
| *Manacus vitellinus* for genome | This paper | BGI_N305 |
| **Recombinant DNA** | | |
| Zebra finch *TLE4* brain cDNA clone (Estima collection; probe) | Clemson University Genomics Institute (CUGI); zebra finch Estima collection | NCBI GenBank: CK306099 |
| Zebra finch *MEIS2* brain cDNA clone (Estima collection; probe) | Clemson University Genomics Institute (CUGI); zebra finch Estima collection | NCBI GenBank: CK314886 |
| **Software and algorithms** | | |
| MaSuRCA v3.1.1 | Zimin et al.[74] | https://github.com/alekseyzimin/masurca |
| MaSuRCA v3.3.8 | Zimin et al.[74] | https://github.com/alekseyzimin/masurca |
| SOAPdenovo2 | Luo et al.[75] | https://github.com/aquaskyline/SOAPdenovo2 |
| Bowtie2 | Langmead and Salzberg[76] | http://bowtie-bio.sourceforge.net/bowtie2/ |
| Pilon | Walker et al.[77] | https://github.com/broadinstitute/pilon |
| TrimGalore! | Felix Krueger, Babraham Bioinformatics | https://www.bioinformatics.babraham.ac.uk/projects/trim_galore/ |
| PBJelly v15.8.24 | English et al.[78] | http://sourceforge.net/projects/pb-jelly/ |
| ALLPATHS2 assembler | MacCallum et al.[79] | N/A (legacy) |
| IMAGE (gap assembly) | Tsai et al.[80] | https://sourceforge.net/projects/image2/ |
| SSPACE | Boetzer et al.[81] | https://github.com/nsoranzo/sspace_basic |
| SuperNova v2.1.1 genome assembler | 10× Genomics | https://github.com/10XGenomics/supernova |
| Progressive Cactus v2019.03.01 | Armstrong et al.[82] | https://github.com/ComparativeGenomicsToolkit/cactus |
| RepeatMasker | Smit et al.[83] | http://repeatmasker.org/ |
| Ragout v2.3 | Kolmogorov et al.[84] | https://github.com/fenderglass/Ragout |
| BWA-mem | Li and Durbin[85] | https://github.com/lh3/bwa |
| bcftools | Li[86] | https://github.com/samtools/bcftools |
| VCFtools | Danecek et al.[87] | https://vcftools.github.io/ |
| pixy | Korunes and Samuk[88] | https://github.com/ksamuk/pixy |
| RagTag | Alonge et al.[89] | https://github.com/malonge/RagTag |
| manakin za analysis scripts | This paper | https://github.com/kfpbennett/manakin_za |
| GATK v3.8.1 | DePristo et al.[90] | https://gatk.broadinstitute.org/hc/en-us |

(*Continued on next page*)

Please cite this article in press as: Balakrishnan et al., Genomic and physiological changes in a sexually selected and frugivorous bird radiation, Current Biology (2026), https://doi.org/10.1016/j.cub.2026.05.021





*Continued*

| REAGENT or RESOURCE | SOURCE | IDENTIFIER |
|---|---|---|
| SnpEff v4.3t | Cingolani et al.[91] | https://sourceforge.net/projects/snpeff/ |
| R v4.0.2 | R Core Team[92] | https://www.r-project.org/ |
| ManacusMK | This paper | https://github.com/periperipatus/ManacusMK |
| NCBI C toolkit | NCBI | https://blast.ncbi.nlm.nih.gov/doc/blast-help/downloadblastdata.html |
| MAFFT | Katoh et al.[93] | https://mafft.cbrc.jp/alignment/software/ |
| pal2nal | Suyama et al.[94] | https://github.com/liaochenlanruo/PAL2NAL |
| ALISCORE | Misof and Misof[95] | https://search.r-project.org/CRAN/refmans/ips/html/ips-package.html |
| ALICUT | Kück et al.[96] | https://github.com/PatrickKueck/AliCUT |
| SWAMP | Harrison et al.[97] | https://github.com/peterwharrison/SWAMP |
| COATS (Creating Orthologous Alignments from Transcriptome Sequences) | This paper | https://hub.docker.com/r/michaelsbrewer/coats_test |
| aBSREL v2.1 | Smith et al.[31] | https://github.com/veg/hyphy-absrel |
| NCBI BLAST+ v2.11.0 | Altschul et al.[98] | https://blast.ncbi.nlm.nih.gov/ |
| DAVID functional annotation clustering v6.8 | Dennis et al.[35]; Huang et al.[36] | https://davidbioinformatics.nih.gov/tools.jsp |
| Geneious Prime | Dotmatics | https://www.geneious.com/ |
| FilterUncorrectabledPEfastq.py | Freedman et al.[99] | https://github.com/harvardinformatics/TranscriptomeAssemblyTools/blob/master/utilities/FilterUncorrectabledPEfastq.py |
| FastQC | Andrews[100] | https://www.bioinformatics.babraham.ac.uk/projects/fastqc/; RRID: SCR_014583 |
| Rcorrector | Song and Florea[101] | https://github.com/mourisl/Rcorrector |
| STAR v2.7.3a | Dobin et al.[102] | https://github.com/alexdobin/STAR |
| R package GEIGER v2.0.6 | Pennell et al.[103] | https://cran.r-project.org/web/packages/geiger/ |
| Muscle5 | Edgar[104] | https://github.com/rcedgar/muscle |
| R packages Phanghorn v2.7.0 | Schliep[105] | https://github.com/KlausVigo/phangorn |
| R packages ape v5.5 | Paradis and Schliep[106] | https://github.com/emmanuelparadis/ape |
| FastML | Ashkenazy et all[107] | https://fastml.tau.ac.il/ |
| TranslatorX webserver | Abascal et al.[108] | http://translatorx.co.uk/ |
| aBSREL (Datamonkey webserver) | Weaver et al.[109] | https://datamonkey.org/absrel |
| RELAX | Wertheim et al.[110] | https://github.com/veg/hyphy-analyses |
| GBLOCKs | Castresana[111] | https://ngphylogeny.fr/tools/tool/276/form |
| Maestro (Schrödinger Suite 2019–1) | Schrödinger | https://www.schrodinger.com/products/maestro |
| R package GenomicFeatures v1.48.4 | Lawrence et al.[112] | https://www.bioconductor.org/packages/release/bioc/html/GenomicFeatures.html |
| R package edgeR v3.38.4 | Chen et al.[113] | https://bioconductor.org/packages/release/bioc/html/edgeR.html |
| PhyDGET | Pease et al.[12] | https://github.com/peaselab/phydget |
| R package phytools | Revell[114] | https://cran.r-project.org/web/packages/phytools/index.html |
| R package corHMM | Beaulieu et al.[115] | https://cran.r-project.org/web/packages/corHMM/index.html |
| R package shiftPlot | Miller and Martin[116] | https://github.com/eliotmiller/shiftPlot |
| R package PhylogeneticEM | Bastide et al.[117,118] | https://cran.r-project.org/web/packages/PhylogeneticEM/ |

(*Continued on next page*)

Please cite this article in press as: Balakrishnan et al., Genomic and physiological changes in a sexually selected and frugivorous bird radiation, Current Biology (2026), https://doi.org/10.1016/j.cub.2026.05.021



*Continued*

| REAGENT or RESOURCE | SOURCE | IDENTIFIER |
|---|---|---|
| Other | | |
| Pacific Biosciences RSII long-read sequencing | Pacific Biosciences | N/A |
| PacBio Sequel long-read sequencing | Pacific Biosciences | N/A |
| 10× Chromium linked-read library preparation | 10× Genomics | N/A |
| Illumina HiSeq 2000 sequencing | Illumina | N/A |
| Illumina HiSeq 2500 sequencing | Illumina | N/A |
| Illumina HiSeq 3000 sequencing | Illumina | N/A |
| Illumina HiSeq 4000 sequencing | Illumina | N/A |
| Illumina HiSeq X sequencing | Illumina | N/A |
| Illumina NextSeq 550 sequencing | Illumina | N/A |
| EltonTraits database | Wilman et al.[69] | N/A |
| Plumage scores | Dale et al.[68] | N/A |
| Breeding system | Tobias et al.[67] | N/A |

## EXPERIMENTAL MODEL AND STUDY PARTICIPANT DETAILS

### Bird specimens for genome sequencing

Manakin samples used for genome sequencing were obtained from museum specimens from the Louisiana State University, Museum of Zoology (LSUMZ) and the Yale Peabody Museum, Vertebrate Zoology, Division Ornithology (YPM MZ ORN) (*Lepidothrix coronata*, LSUMZ B3197, from voucher specimen #110521; *Pipra filicauda*, LSUMZ B4331, from voucher specimen #115617; *Neopelma chrysocephalum*, YPM-ORN-139661) or were collected under local permits (*Manacus vitellinus*; permits approved by the Autoridad Nacional del Ambiente and the Autoridad del Canal de Panamá to Barney Schlinger, and *Corapipo altera*, collected in Costa Rica Rica by Elsie Shogren and Alice Boyle under permits from the Ministerio del Ambiente y Energía (MINAE), Comisión Nacional para la Gestión de la Biodiversidad Oficina Técnica and the Ministerio del Ambiente y Energía (MINAE), Sistema Nacional de Áreas de Conservación; partial voucher specimen accessioned at Kansas State University collection, #K-1909).

### Specimens for transcriptomics

Transcriptomes were sequenced from *Manacus vitellinus* (one individual; from kidney, brain, liver; PRJNA320632), *Lepidothrix coronata* (one individual; liver, testis, muscle, PRJNA321179), and *Pipra filicauda* (tissues from four individuals: testes, ventromedial hypothalamus (VMH), arcopallium intermedium (AI); SRR6811833-SRR6811838, used in a previous study[119]) to improve genome annotation. Additional tissues for transcriptome sequencing for kidney, liver, and digestive tract from three golden-collared manakins (*Manacus vitellinus*) were obtained from three wild-caught individuals collected by Lainy Day in Gamboa, Panamá (BioProject PRJNA892803). *Manacus* and *Lepidothrix* individuals used for transcriptomes were collected under permits from the Autoridad Nacional del Ambiente, and the Autoridad del Canal de Panamá to Lainy Day and Matthew Fuxjager. Muscle tissue transcriptomes from six manakins and a tyrant flycatcher (*Mionectes oleagineus*) were obtained from a published study.[12]

### Population resequencing and RADseq

RADseq data for Z:autosome nucleotide diversity calculations were downloaded from the following GenBank BioProjects: 11 *Rhegmatorhina berlepschi* samples, BioProject PRJNA763942, specifically SRR35754672, SRR35754673, SRR35754695, SRR35754696, SRR35754717, SRR35754738, SRR35754748, SRR35754760, SRR35754777, SRR3575480, SRR35754834[120]; 13 *Empidonax alnorum* samples, BioProject PRJNA692615, specifically SRR14848188, SRR14848190, SRR14848302, SRR14848303, SRR14848310, SRR14848313, SRR14848314, SRR14848315, SRR14848318, SRR14848320, SRR14848321, SRR14848322, SRR14848333[121]; 20 *M. vitellinus* samples, BioProject PRJNA893627, specifically SRR22133426, SRR22133437, SRR22133438, SRR22134030, SRR22134035, SRR22134037, SRR22134038, SRR22134058, SRR22134059, SRR22134070, SRR22134093, SRR22143061, SRR22143084, SRR22143106, SRR22143115, SRR22143117, SRR22143121, SRR22143124, SRR22158168, SRR22158173[122]; two *P. filicauda* samples, BioProject PRJNA837991, specifically SRR19417635 and SRR19417717 from[123] and six *L. coronata* samples, BioProject PRJNA787238, specifically SRR17237521, SRR17237542, SRR17237543, SRR17237574, SRR17237576, SRR17237584 from.[124] RADseq data for *Corapipo altera* (33 males) were obtained from DNA extracted from blood samples in Costa Rica by Shogren[72] and Alice Boyle under permits from the Ministerio del Ambiente y Energía (MINAE), Comisión Nacional para la Gestión de la Biodiversidad Oficina Técnica (R-024-2016-OT-CONAGEBIO) and Ministerio del Ambiente y Energía (MINAE), Sistema Nacional de Áreas de Conservación (SINAC-SE-CUS-PI-R-032-2016). RADseq data for *Neopelma chrysocephalum* were obtained from DNA extracted from tissue samples from specimens collected between 1999 and 2001 and accessioned into the Smithsonian National Museum of Natural History, catalogue numbers 627212, 627076, 659093, 659094, 625577, 625578, and 625576. Resequencing data from *Manacus candei* was generated from genomic DNA derived from specimens collected between 1991 and 1997 and accessioned into the

Please cite this article in press as: Balakrishnan et al., Genomic and physiological changes in a sexually selected and frugivorous bird radiation, Current Biology (2026), https://doi.org/10.1016/j.cub.2026.05.021





Smithsonian National Museum of Natural History: 22 samples were used in the McDonald-Kreitman selection testing analysis (B04590, B01878, B01883, B01884, B01886, B01888, B01890, B01891, B01894 B01921, B01922, B01924, B01897, B01898, B01899, B01903, B01908, B01909, B01910. B01911, B01948, B01949).

### Gene cloning and functional assay samples

For *T1R* amplification from *Lepidothrix coronata* and *Neopelma chrysocephalum*, tissue samples from the Louisiana State University, Museum of Zoology were used (*Lepidothrix coronata*: LSUMZ B3197; *Neopelma chrysocephalum*: LSUMZ B25410). Draft genomic data for a rusty-margined flycatcher (GCF_022539395.1) (generated for another project) from an individual collected in Brazil (collection permit #30319-1 issued to Dr. Maria Luisa da Silva, Federal University of Para, Belem, Brazil; Genetic Patrimony #A980A63) was mined to obtain sequence information for *LPH* (lactase-phlorizin).

### Tissue samples for in situ hybridization

For brain expression analysis, we used sections from the zebra finch brain section collection kept in the Mello lab at Oregon Health and Science University (OHSU), Portland, OR, USA. These sections were previously obtained from adult male zebra finches bred and maintained under procedures approved by OHSU's Institutional Animal Care and Use Committee and in accordance with NIH guidelines. The brain of a red-headed manakin (*Ceratopipra rubrocapilla*) was obtained in 2011 in the context of collection of bird specimens for the Museu Paraense Emilio Goeldi (MPEG; Belem, PA, Brazil), under its ornithology curator Dr. Alexandre Aleixo.

## METHOD DETAILS

### Genome sequencing and assembly

For all assemblies, contaminating contigs, library adaptors, ambiguous bases (i.e., Ns) in the sequence and contigs < 200 bp were removed prior to submission to NCBI. Details on individual assemblies are listed below.

#### *Manacus vitellinus*, *Pipra filicauda*

The *Manacus vitellinus* assembly (GCA_001715985.3) has a contig N50 of 0.29 megabases (mb) and a scaffold N50 of 17.9 mb. The first *M. vitellinus* genome (GCA_000692015.2) was originally sequenced as part of the Avian Phylogenomics Project[125] with short read paired-end and mate-pair libraries (NCBI BioProject: PRJNA212872). In order to improve its contiguity, we used Pacific Biosciences RSII long read sequencing to supplement the short-read data. After obtaining ~12x long read data, we assembled the genome using a hybrid assembly approach based on "mega reads" that is incorporated into the assembly software, MaSuRCA 3.1.1.[74] The assembled contigs were then scaffolded with the SOAPdenovo2 scaffolding module using mate-pair data.[75] During our initial analyses using this genome, we identified a few areas where errors in the consensus sequence persisted so we used the Illumina paired-end reads to polish the assembly. To do that, we first mapped the reads back to the assembled genome using Bowtie2,[76] then we used Pilon to error-correct the genome based on the alignment.[77]

For the *Pipra filicauda* genome (GCA_003945595.2; contig N50 1.6 mb, scaffold N50 2.5 mb) we also used a hybrid approach, here combining deep Illumina sequencing (~100x) with ~20x PacBio Sequel long-reads. We trimmed the Illumina data with TrimGalore! (https://www.bioinformatics.babraham.ac.uk/projects/trim_galore/), then assembled the genome using MaSuRCA 3.3.8. Following assembly, we used PBJelly 15.8.24 with the PacBio Sequel reads for further gap filling.[78] Bowtie2 and Pilon were then used for error correction.

#### *Lepidothrix coronata*

For *Lepidothrix coronata*, (GCA_001604755.1, contig N50 0.14 mb, scaffold N50 5 mb), Illumina data was used and assembled following the ALLPATHS2[79] assembler guidelines. This approach requires 45x sequence coverage of each fragment (overlapping paired reads ~180 bp length) from 3 kb paired end (PE) reads as well as 5x coverage of 8 kb PE reads. All sequences were generated on an Illumina HiSeq2500. The combined sequence reads were assembled using ALLPATHS2 software and where possible, scaffold gaps were closed by mapping with 30X coverage of Illumina sequences (~180 bp fragments) and local gap assembly using IMAGE.[80] The same source long insert reads (3 and 8 kb PE) were used to further extend assembled scaffolds using SSPACE.[81]

#### *Neopelma chrysocephalum*, *Corapipo altera*

The assemblies for *N. chrysocephalum* (GCA_003984885.2; contig N50 0.24 mb, scaffold N50 10.5 mb) and *C. altera* (GCA_003945725.1, contig N50 0.26 mb, scaffold N50 12.4 mb) were generated using the 10× Chromium platform. High molecular weight DNA extractions, 10× Chromium library preps and Illumina HiSeq X sequencing (1 lane each) were conducted at the Hudson Alpha Institute for Biotechnology. The linked reads were assembled using SuperNova version 2.1.1. Assemblies were generated targeting 56x coverage (a subset of the total data) following the manufacturer's instructions for optimum assembly.

### Genome annotation

After accession into GenBank, assemblies were repeat-masked and annotated by NCBI using the GNOMON pipeline (see https://www.ncbi.nlm.nih.gov/genome/annotation_euk/gnomon/ for a full description of the NCBI gene annotation pipeline). Transcriptomes were

sequenced from *Manacus* (from kidney, brain, liver), *Lepidothrix* (testes, muscle, liver), *Pipra* (testes, brain) and uploaded to NCBI (accessions:PRJNA320632, PRJNA321179 and PRJNA437157) to improve gene model accuracy.

## Genome alignment and chromosome assignment

ProgressiveCactus v2019.03.01[82] was used to align the assembled genomes of *Manacus*, *Corapipo*, *Lepidothrix*, *Empidonax*, *Neopelma*, and *Pipra*, with *Taeniopygia guttata* (GCA_003957565.4) included as an outgroup. All genomes were softmasked using RepeatMasker[83] with 'chicken' as the reference genome before alignment and a star tree was used as input. The resulting hal alignment file was used to determine chromosome assignments using Ragout v2.3[84]; *Taeniopygia guttata* was the reference genome upon which scaffolds were assigned to chromosomes. Z-chromosome associated alignments were then extracted from the hal file after converting it to a MAF (multiple alignment file) based on Ragout chromosome assignments. These were filtered to exclude ancestral sequence reconstructions and non-orthologs during the hal to MAF conversion (only orthologous sequences were included).

## Genetic diversity and Z/A diversity ratios

To calculate ratios of nucleotide diversity on the Z chromosome relative to autosomes, we obtained restriction site-associated DNA sequencing (RADseq) data from population samples of *M. vitellinus*, *P. filicauda*, *L. coronata*, *C. altera*, *N. chrysocephalum*, and two non-manakin suboscine outgroups: *Empidonax alnorum*, a flycatcher in Tyrannida, and *Rhegmatorhina berlepschi*, an antbird in Furnariida. All tissue or blood samples were obtained from males in a single geographic locality (or, in the case of *N. chrysocephalum* and *L. coronata*, a set of nearby localities. For *M. vitellinus*, *P. filicauda*, *L. coronata*, *E. alnorum*, and *R. berlepschi*, we downloaded raw sequencing reads from GenBank (respective accession numbers: PRJNA893627, PRJNA837991, PRJNA787238, PRJNA692615, and PRJNA763942). *N. chrysocephalum* DNA was isolated from frozen tissues using phenol:chloroform extraction. *M. vitellinus* (n = 20) and *N. chrysocephalum* (n = 7) libraries were prepared using a single SbfI digest and sequenced on 2x150 bp lanes of an Illumina HiSeq 4000. *P. filicauda* libraries (n = 2) were prepared using a single PstI digest and single-end sequenced to 70 or 100 bp on an Illumina HiSeq 2000 lane.[123] *L. coronata* libraries (n = 6) were prepared using NheI and EcoRI digestions and sequenced across three 2x150 bp lanes on an Illumina HiSeq X[77]. *R. berlepschi* libraries were prepared using XbaI and EcoRI digestions and sequenced in 2x150 bp reads on an Illumina HiSeq 3000.[120] *E. alnorum* libraries were prepared using PstI and MspI digestions and sequenced in 2x100 bp reads on an Illumina HiSeq 2500 and HiSeq 4000.[121] For *C. altera*, blood was collected in the field (n = 33). DNA was digested with BtgI and TaqI and sequenced on four 1x150 bp lanes of a NextSeq 550 High-Output FlowCell (Illumina, USA). We mapped reads from each species to its own genome (Figure 1E) using BWA-mem[85] with default settings. In the case of *R. berlepschi* and *E. alnorum*, we mapped reads to the reference genomes for their sister species, *R. hoffmannsi* (Accession LSU_RhHo_2.0) and *E. traillii* (ASM303162v1). Sequencing depth was as follows: *R. berlepschi*, 64.6X (with a range per sample of 44.1-92.9X); *E. alnorum*, 8.0X (3.9-15.9X); *N. chrysocephalum*, 19.9X (11.2-26.9X); *C. altera*, 10.9X (4.9X-16.5X); *L. coronata*, 51.9X (37.3-67.9X); *M. vitellinus*, 21.6X (7.7-71.1X); and *P. filicauda*, 7.9X (7.7-8.1X). We called SNPs and produced an all-sites VCF file using bcftools mpileup and bcftools call[86] with default settings then filtered VCFs using VCFtools[87] to retain only sites that were present in $\geq$ 75% of the samples in *R. berlepschi*, *E. alnorum*, *C. altera*, and *M. vitellinus* samples, 70% of *N. chrysocephalum* samples, and 65% of *L. coronata* samples. We calculated nucleotide diversity ($\pi$) using default settings in pixy.[88] To obtain the corresponding chromosome from scaffolds in each genome assembly, we ran RagTag[89] scaffold with default settings for each genome to the chromosome-level assembly of *Chiroxiphia lanceolata* (bChiLan1.pri). We calculated Z/A diversity ratios by summing per chromosome the quotient of pairwise nucleotide differences by the number of comparisons available (i.e., calculating chromosome pi), and dividing this value for the Z chromosome by each autosome. We confirmed that qualitative results were unaffected by the choice of reference genome by subsequently mapping all reads to *M. vitellinus* and recalculating nucleotide diversity (Figure S1). Scripts used for these analyses are available at https://github.com/kfpbennett/manakin_za.

## MK test using resequencing data

We used the McDonald-Kreitman (MK) test of positive selection in the *Manacus* lineage using whole genome re-sequencing data and variant calls for *M. candei*, generated for another project on the *Manacus candei* x *vitellinus* hybrid zone[33]; *M. candei* and *M. vitellinus* are closely-related species that are similar in morphology as well as in courtship and display behavior.[15,126,127] We chose *M. candei* samples rather than *M. vitellinus* samples to maximize sample sizes and chose populations of *M. candei* that would minimize the influence of introgressed alleles. The MK test is based on the ratio of non-synonymous and synonymous changes that are polymorphic and fixed with respect to an outgroup lineage (*Pipra filicauda*; reads were obtained from the assembly generated here (SRR6885520)). Whole genome resequencing data was generated from 22 *M. candei* individuals from three localities along the hybrid-zone transect in NW Panama (populations 2 (n = 2), 3 (n = 10) and 4 (n = 10).[33] Reads from the *Pipra filicauda* and *Manacus* samples were processed with a similar pipeline (see also[33]): an average of 97.6 million paired-end reads (150bp) were obtained per *Manacus* individual, and the trimmed reads were aligned to the *Manacus vitellinus* reference genome (ASM171598v3) using Bowtie v 2.3.5.[76] SNPs and indels were called for *Manacus* and *Pipra* using GATK v3.8.1 with the HaplotypeCaller function, and subsequently filtered at the SNP and genotype level using VariantFiltration.[90]

For the MK test, we filtered the variant call format (VCF) file to only include *M. candei* and *P. filicauda*, and subsequently filtered with VCFtools to include only biallelic sites.[87] We used SnpEff v 4.3t[91] to annotate the sites within the VCF file as synonymous or non-synonymous changes using the *Manacus vitellinus* gene annotations (Annotation Release 103, NCBI RefSeq assembly accession

Please cite this article in press as: Balakrishnan et al., Genomic and physiological changes in a sexually selected and frugivorous bird radiation, Current Biology (2026), https://doi.org/10.1016/j.cub.2026.05.021





GCF_00175985.3). Across all the *M. vitellinus* coding sequences (CDS) there were 437064 sites across 13,827 genes, with individuals missing between 0.14%-14.01% sites. Sites that were missing in the *P. filicauda* individual were excluded from downstream analysis, leaving 434,449 sites for analysis. We used a custom script to process the VCF and run the MK test in R v 4.0.2[92] (see https://github.com/periperipatus/ManacusMK). We determined excesses of polymorphic or fixed non-synonymous differences using a Fisher's exact test, and the neutrality index (NI) was calculated to determine the ratio of nonsynonymous to synonymous changes per gene. For plotting NI, zero counts were replaced with one, and the NI was -log10 transformed, so negative values represent negative selection and positive values represent positive selection.[128]

### MK results and muscle expression data

To determine whether some genes under selection in *Manacus* also show changes in gene expression, we compared selection signatures from the MK test with expression changes described in a previous study that examined gene expression changes associated with rapid wing displays in *Manacus* and *Ceratopipra* manakins.[12] Among the list of genes significant in the MK test, 4 unique genes showed phylogenetic evidence (Bayes Factor > 0.4) for expression change in the scapulohumeralis (SH) muscle in *Manacus* (*UTP20*, *JPH2*, *ADPRH*) and/or independently in *Manacus* and *Ceratopipra* (*UTP20*, *ADPRH*, *SCN4A*). Two of these, JPH2 and SCN4A, have well-described functions in muscle performance and showed significant expression differences between *M. vitellinus* and *L. coronata* and *Pseudopipra pipra* manakins (ANOVA, R aov function, post hoc, Tukey test $p < 0.01$).

### Lineage-specific selection tests on genes

We aligned NCBI-generated (GNOMON) gene predictions from five manakin genomes and five outgroups (two songbirds, *Ficedula albicollis* (GCF_000247815.1_FicAlb1.5), *Corvus cornix* (GCF_000738735.2_ASM73873v2); a tyrant flycatcher *Empidonax traillii* (GCF_003031625.1_ASM303162v1); and an eagle and a parrot, *Aquila chrysaetos* (GCF_900496995.1_bAquChr1.2), and *Melopsittacus undulatus* GCF_000238935.1_Melopsittacus_undulatus_6.3) to test for signatures of selection among manakins. Putative orthologs were identified by reciprocal blast of predicted amino acid sequences (blastall -p blastp, -e 1-20)[129] from each species against *M. vitellinus*. The associated DNA sequences were then aligned in a "codon aware" manner using MAFFT[103]and pal2nal.[94] The resulting alignments were refined (trimming regions of poor alignment quality) using the programs ALISCORE[95] and ALICUT[96] and SWAMP.[97] The pipeline for these alignment and filtering steps (COATS: Creating Orthologous Alignments from Transcriptome Sequences) is available as a docker repository (https://hub.docker.com/r/michaelsbrewer/coats_test) and the default settings in the associated scripts were used throughout. We tested for selection using adaptive branch-site random effects likelihood (aBSREL) (version 2.1)[31] using the species tree, and examining the nodes that encompass 1) all of the suboscines 2) Pipridae and 3) Piprinae (see *Tests of positive and relaxed selection* below for further details of tests on LPH).

### Refining poorly annotated gene symbols

Annotations of *Pipra filicauda* genes were used to initially define gene symbols for each orthogroup. For the *Pipra* genes without gene symbols annotated (for instance, genes with a locus (LOC) number), we employed an iterative reciprocal-BLAST based strategy. First, we blasted the *Pipra* genes against the human and three annotated manakin genomes (two from this study, *Lepidothrix coronata* and *Neopelma chrysocephalum* as well as the lance-tailed manakin *Chiroxiphia lanceolata*) using the "blastn" program (-task megablast -db nt -evalue 0.01) in the NCBI-BLAST software, version 2.11.0.[98] We compared the BLAST results from each query gene. If all hits had the same gene symbol, this was extracted and used to annotate the query *Pipra* gene. If reciprocal BLASTing returned multiple hits with different information, we chose the gene symbol whose description matches the description of the best hit (highest score value), otherwise, the gene symbol that appeared most frequently (and for this round, was present in both genomes) was selected. Next, the *Pipra* genes for which we were unable to obtain a gene symbol were blasted again using the same procedure against an extended second set of well-annotated bird species (chicken, great tit, collared flycatcher, and zebra finch), and then against annotations from all birds and reptiles.

### Enrichment of positively-selected genes

#### *DAVID enrichments at suboscine nodes*

To identify functional pathways associated with positively selected genes in manakins, we examined the sets of positively selected genes from aBSREL tests at the target nodes within suboscines (genes exhibiting positive selection on the ancestral branch leading to the suboscine, Pipridae and Piprinae clades, as well as the set of positively selected genes from the McDonald-Kreitman test (selection in *Manacus* relative to *Pipra*)). For aBSREL and the MK test, the enrichment analysis was done relative to a background of 9,436 genes aligned across 10 species, and 13,826 genes, respectively.

For the positively-selected gene sets, we used the Database for Annotation, Visualization, and Integrated Discovery (DAVID[35,36]) to test for enrichment (using different databases including Gene Ontology and KEGG functional annotations). This is a foreground/background test, and genes with unique gene symbol annotations with uncorrected $p < 0.05$ were considered foreground (*Manacus* = 113, from the MK test, as well as Piprinae = 155, Pipridae = 301, suboscine = 653) and all genes (with unique gene symbol annotations) considered in the selection tests were considered background (for aBSREL tests, 8766 genes with unique gene symbol annotations; for MK tests, 13074). DAVID analyses included Gene Ontology (Molecular Function, Biological Process and Cellular Component), UniProt Keyword, and Kyoto Encyclopedia of Genes and Genomes (KEGG) databases. DAVID outputs statistics for terms with uncorrected $p < 0.1$ (Manacus = 57, Piprinae = 44, Pipridae = 84, suboscines = 173) and calculates an enrichment metric based on the

Please cite this article in press as: Balakrishnan et al., Genomic and physiological changes in a sexually selected and frugivorous bird radiation, Current Biology (2026), https://doi.org/10.1016/j.cub.2026.05.021



number of genes associated with a particular term in the foreground relative to the background. Examination of DAVID results after Bonferroni correction showed enrichment of only a small number of terms (5; FDR correction yields similar number of terms), including immune-related GO terms (as expected[130]), and within Pipridae, genes related to protein digestion and absorption. We next examined GO-terms with weaker enrichment signals ($p < 0.05$ before multiple correction), and observed enrichment of terms related to 5 broad categories relevant to manakin biology (diet/taste, muscle, visual/auditory sensory systems, sperm, and telomeres, Table S1). These included genes related to diet, which were enriched both in suboscines and in manakins (genes related to digestion, absorption, and transport of carbohydrates, lipids, and proteins as well as genes related to intestinal morphology and to insulin release), muscle-related genes (enriched in manakins), as well as genes related to vision (suboscines), telomeres (enriched in Piprinae and *Manacus* tests, related perhaps to overabundance of reactive oxygen species (ROS) from high athleticism[42,131]), and sperm (in the McDonald-Kreitman tests).

Next, we expanded beyond the list of enriched GO-terms and included additional terms related to the 5 broad categories, and queried the list of positively-selected genes for genes associated with these terms in all tested branches (Table S2). Alignments of genes associated with these traits were then manually inspected, and, subsequently, predictions of four additional suboscines were added to these sets and aBSREL tests were conducted (Figure 2E).

#### *Curation of alignments with expanded taxa*

For a subset of target candidate genes (most determined using the GO enrichment analyses described above) predictions from four additional outgroups (the Old World suboscine representative, African broadbill (*Smithornis capensis*, ASM1339646v1), a member of Furnariida, the white-breasted antbird (*Rhegmatorhina hoffmannsi*, GCA_013398505.2), a cotinga, the Amazonian umbrellabird (*Cephalopterus ornatus*; ASM1339677v1), and an additional member of Tyrannida, the wing-barred piprites (*Piprites chloris*; ASM1339929v1)) were added to pinpoint the timing of selection signatures within suboscines. For taxa missing predictions from the antbird, sequences from the band-tailed hornero (*Furnarius figulus*: ASM1339746v1) were substituted. To start, automated predictions (annotations from the 10,000 Bird Genomes (B10K) project) were used[132]; when these were missing or substantially shorter than the original alignment, predictions were manually curated by standalone BLAST using exons from *Lepidothrix coronata* as query sequences. The sequences of these additional taxa were aligned to the trimmed alignment from the original 10-taxon set and corresponding regions were trimmed; in some instances, poorly-aligned regions were removed. For some loci, predictions from the original 10-taxon set were also manually curated (for instance where the original trimmed alignment was severely truncated relative to the new predictions). Manual curation of some loci, such as taste receptors, visual opsins and melanopsins was conducted by aligning individual exons to their predicted genomic contig or scaffold location using Geneious Prime, and confirming the location of each splice site at the 5' and 3' end of each exon. aBSREL branch tests were run on the curated alignments and signatures of selection were examined at three target branches leading up to the manakin radiation (Figure 2D): before the divergence of manakins, tyrants and cotingas (the common ancestor of the Tyrannida clade); before the manakin clade (Pipridae), and after *Neopelma* (before Piprinae).

### RNA-seq of liver, kidney, gut, and muscle

RNA from three tissue types from three golden-collared manakins was extracted and libraries were prepared using NEBNext Ultra II RNA Library Preparation Kit after rRNA depletion using Qiagen Fastselect (GENEWIZ). Illumina sequencing data from three individuals (two adult females and one juvenile) were analyzed for liver, intestine and kidney. We processed short reads following Freedman et al.[99] Briefly, after an initial assessment of sequence read quality with FastQC (http://www.bioinformatics.babraham.ac.uk/projects/fastqc/),[100] we performed kmer-based error correction with Rcorrector,[101] discarded read pairs if one read was unfixable using a python script (https://github.com/harvardinformatics/TranscriptomeAssemblyTools/blob/master/utilities/FilterUncorrectabledPEfastq.py), and trimmed adapters and low-quality reads with TrimGalore (https://www.bioinformatics.babraham.ac.uk/projects/trim_galore/)(setting the minimum phred quality score to 33, the minimum post- trimming read length to 36, and the adapter filtering stringency parameter to 5). We further removed reads mapped to rRNAs present in the SILVA dataset (the SSU Parc and LSU Parc sets, release 132) using bowtie2. A second run of Fastqc was used to confirm that there was no remaining adapter sequence in the filtered reads. The kidney sample from the juvenile was discarded after filtering due to insufficient read retention.

We next conducted splice-aware mapping of the filtered reads to the manakin reference genome (GCF_001715985.3). The genome was indexed using STAR version 2.7.3a[102] with the option –sjdbOverhang set to 99. Read mapping was conducted with STAR with created indices and the reads per gene were estimated during the mapping process using the option –quantMode GeneCounts (–sjdbGTFfile was set to GCF_001715985.3_ASM171598v3_genomic.gtf.

### UCNE analysis

#### *Identification of manakin-divergent UCNEs*

4,351 ultra-conserved noncoding element (UCNE; noncoding sequences highly conserved throughout vertebrate phylogeny) consensus sequences from chicken were retrieved from UCNEbase.[73] Orthologous UCNEs were identified in all 5 manakin genomes presented in this study, as well as 17 outgroup species where high-coverage genomes were available. These included *Empidonax traillii*[133]; *Piprites chloris*, *Cephalopterus ornatus*, *Rhegmatorhina hoffmannsi*, and *Smithornis capensis*[132]; *Taeniopygia guttata*[134]; *Amazona aestiva*[135]; *Melopsittacus undulatus*, *Nestor notabilis*, *Falco peregrinus*, *Picoides pubescens*, *Nipponia nippon*, *Opisthocomus hoazin*, *Columba livia*, *Anas platyrhynchos*, and *Struthio camelus*.[136] Orthologous UCNEs across species were obtained by aligning the chicken UCNE set[73] to each genome using BLAST with parameters -blastn -dust no -evalue 0.01 -max_

Please cite this article in press as: Balakrishnan et al., Genomic and physiological changes in a sexually selected and frugivorous bird radiation, Current Biology (2026), https://doi.org/10.1016/j.cub.2026.05.021





target_seqs 1 -max_hsps 1. As UCNEs are defined as non-coding regions > 200bp with ≥ 95% sequence identity between human and chicken, we considered UCNEs that exhibited a ratio of mismatches to total sequence length of 5% or more to be divergent. In order to identify UCNEs specifically divergent in the manakin lineage, we implemented the phylogenetic ANOVA in the R package GEIGER v2.0.6,[103] using the species tree from the avian phylogenomics consortium[136] (updated following[51] to include additional taxa), 1,000 in silico simulations, and a phylogenetically corrected significance threshold of $\alpha < 0.05$. We identified a set of 99 UCNEs with significant sequence divergence in manakins relative to other avian genomes (see Table S3).

### Relative timing of UCNE changes

We next performed two different types of analyses using the set of divergent UCNEs in manakins. First, to examine the relative timing of changes within the manakin clade, we realigned UCNE loci with MUSCLE[104] (v5, default settings). We pruned alignments to include only the passerines + parrot clade. In order to accurately polarize changes at the base of the manakin clade, we required that all three parrots, zebra finch, and four of the non-manakin suboscines were included in the alignment, in addition to all five manakins. We then used the R packages Phanghorn[105] (v 2.7.0) and Ape[106] (v5.5) to derive parsimony-based (acctran function in Phanghorn) reconstructions of substitutions along the tree topology. Next, we tallied the number of changes in each of the divergent elements that evolved on the branch leading to all manakins (including *Neopelma*), as well as the number of changes that occurred on the subsequent branch leading to Piprinae manakins. To examine elements that exhibited more change in Piprinae vs. Pipridae (and thus which may be associated with elaborated traits in the Piprinae clade), we created an index ranging between -1 and 1, by calculating ((#changes in Pipridae)- (#changes unique to Piprinae))/((#changes in Pipridae )+(#changes unique to Piprinae)); elements with values > 0 were categorized as having more changes in Pipridae, and elements with an index value of < 0 as having more changes in derived manakins (Figures 2C and S2; Table S3).

### Enrichment of genes near divergent UCNEs

UCNEs are often associated with enhancers that play critical, conserved roles in development.[73] Using the closest gene (as identified in Dmitrieva and Bucher,[73] [Table S3]) to each of the UCNEs that were divergent in manakins, we performed enrichment analysis in DAVID[35] to examine whether these UCNEs were found close to genes with similar functions. Manakin-divergent UCNEs were proximal to genes enriched for functional terms associated with transcriptional regulation suggesting the possibility that changes to these UCNEs in the manakin lineage could affect the expression of key transcription factors and therefore influence several phenotypes. Several of these genes were proximal to not one, but clusters of multiple manakin-divergent UCNEs, in particular *NR2F1* with 10 and *TLE4* with 7 proximal manakin-divergent UCNEs. Both NR2F1 and TLE4 are known to be involved in the development of the visual system,[46,47] along with several other genes adjacent to manakin-divergent UCNEs, including *MEIS2*, *PAX6*, *PBX3*, *POU6F2*, and *ISL1* (see Table S3). Interestingly, TLE4 and MEIS2 are known to interact in the development of the tectum, a brain region critically involved in motion detection in the visual processing pathway and head/eye orienting responses, and which has been implicated among other things in prey capture.[46,48,49] Given the potential role of the optic tectum in a bird's ability to perceive high-speed courtship dances, we sought to experimentally assess the expression of TLE4 and MEIS2 in the avian optic tectum. We examined both the zebra finch (*Taeniopygia guttata*), a songbird for which resources like a large collection of brain-expressed ESTs and brain gene expression atlas (www.zebrafinchatlas.org; described in Lovell et al.[137]) are available, and the red-headed manakin (*Ceratopipra rubrocapilla*, for which brain sections were available in the Mello lab) for *in situ* hybridization analysis.

### In situ hybridization

To confirm that both *TLE4* and *MEIS2* genes were expressed in the avian optic tectum, we performed non-radioactive *in situ* hybridization on brain sections (10 μm thickness) of optic tectum of an adult male zebra finch and red-headed manakin following a previously described and validated non-radioactive protocol.[137] For probes, we used brain cDNA clones from the zebra finch Estima collection (NCBI clones CK306099 for *TLE4* and CK314886 for *MEIS2*); sequence specificity was examined by BLAST alignments of clone sequences with the zebra finch and manakin genomes in NCBI and verifying correct and unique alignments to loci of interest. Selected clones were grown overnight, and plasmids were isolated (QIAprep Spin MiniPrep Kit), digested with BssHII, and purified (QIAquick PCR purification kit). Digoxygenin(DIG)-labeled antisense riboprobes were synthesized using T3 RNA polymerase (Promega) and a DIG RNA labeling mix (Roche) for 2 h at 37 °C. Riboprobes were purified using Sephadex G-50 columns and stored at 20 °C. Slides were acetylated for 10 min in 1.35% triethanolamine and 0.25% acetic anhydride, briefly washed in 2X SSPE (300 mM NaCl, 20 mM NaH2PO4-H2O) and dehydrated in an ethanol series. Hybridization solution (50% formamide, 2X SSPE, 2 μg/μL tRNA, 1 μg/μL BSA, 1 μg/μL Poly A, and 2 μL DIG-labeled riboprobe in DEPC-treated H2O) was added, and slides were coverslipped and hybridized in a mineral oil bath overnight at 65 °C. After washes in chloroform (to remove oil) and in SSPE (to remove coverslips), slides were washed in 50% formamide 2X SSPE solution followed by two 30 min washes in 0.1X SSPE at 65 °C, agitated every 10 min. Sections were then briefly permeabilized in TNT (100 mM Tris–HCl pH 7.4, 150 mM NaCl, 0.3% Triton X-100), blocked in TNB (100 mM Tris–HCl pH 7.4, 150 mM NaCl, 0.36% w/v BSA, 1% skim milk) for 30 min in a humidified chamber at room temperature, and incubated in an alkaline phosphatase conjugated anti-DIG antibody (Roche Cat# 11093274910; RRID: AB_2313640, 1:600) in TNB for 2 h in a humidified chamber at room temperature. Slides were then washed twice for 15 min in TMN (100 mM Tris–HCl, 150 mM NaCl, 5 mM MgCl2) and incubated for 1–3 days in filtered BCIP/NBT Substrate Solution (PerkinElmer) at room temperature. Slides were then rinsed in DI water, fixed in 3% paraformaldehyde, and washed again in DI water. Slides were coverslipped with VectaMount permanent mounting medium (Vector). Processing was performed in parallel with slides hybridized with no probe (negative control), or with other probes with known expression pattern (e.g. GAD2; positive controls).

We observed layer-specific expression (*TLE4* in superficial retino-recipient layers, and *MEIS2* in the *stratum griseum centrale* (SGC), which contains motion sensitive cells and from which the main tectofugal projection originates) in both species

Please cite this article in press as: Balakrishnan et al., Genomic and physiological changes in a sexually selected and frugivorous bird radiation, Current Biology (2026), https://doi.org/10.1016/j.cub.2026.05.021



(Figures S2A–S2C). Considering the avian optic tectum involvement in visual motion detection and head-orienting reflexes, the expression of *TLE4* and *MEIS2* suggests potential roles in manakins' perceptual abilities related to sexually-selected courtship dances.

## Ancestral reconstruction and selection tests

### Ancestral reconstruction and synthesis

Ancestral reconstruction of T1Rs was performed as recently described[51,52,138] using a maximum likelihood approach in FastML (Yang model of evolution, codon-based reconstruction).[107] Input for the reconstructions consisted of a phylogeny corresponding to the best known species tree, as well as multiple sequence alignments for *T1R1* and *T1R3* (31 species: the same taxa used in ancestral reconstruction in Toda et al.,[51] together with sequences from *Empidonax traillii* and the five manakins sequenced here) as well as for *LPH* (37 species, from publically-available genomes as well as from a draft assembly of the rusty-margined flycatcher). For *LPH*, sequences from the same set of species were used for ancestral reconstruction and testing for relaxed selection (below), including the 14 species used in selection tests in Figure 2, as well as *Struthio camelus*, *Anas platyrhynchos*, *Coturnix japonica*, *Gallus gallus*, *Columba livia*, *Balearica regulorum*, *Aptenodytes forsteri*, *Egretta garzetta*, *Athene cunicularia*, *Haliaeetus leucocephalus*, *Cariama cristata*, *Strigops habroptilus*, *Falco peregrinus*, *Falco cherrug*, *Myiozetetes cayanensis*, *Corvus brachyrhynchos*, *Pseudopodoces humilis*, *Cyanistes caeruleus*, *Parus major*, *Catharus ustulatus*, *Camarhynchus parvulus*, *Serinus canaria*, and *Zonotrichia albicollis*. Alignments were generated using the MAFFT alignment algorithm[93] implemented on the TranslatorX webserver.[108] Insertions and deletions were manually curated from the marginal reconstructions and predicted ancestral sequences were synthesized (GENEWIZ).

### Tests of positive and relaxed selection

Tests of positive selection using aBSREL were conducted on the Datamonkey webserver[109] for the extended alignment of *LPH* (Figure 4B). For the clades where positive selection was identified using aBSREL, further tests were conducted using RELAX[110] (on an alignment trimmed using GBLOCKs[111]) to determine if the signal was due to positive or relaxed selection. Four different tests were conducted, with the foreground branches being set as (a) the node leading to Cotingidae and Tyrannidae, (b) the node leading to Pipridae, (c) the node leading to passerines, and (d) the node leading to Galliformes; the background branches were chosen as branches that were not identified as selected by aBSREL, and were the same for all tests, including the ostrich, duck, pigeon, crane, penguin, egret, the burrowing owl, and the peregrine and saker falcon. The direction and strength of selection is expressed by the parameter K, with low values ($< 1$) indicating relaxed selection and high values ($> 1$) indicating selection intensification. The four different tests were each repeated ten times, as RELAX is known to yield slightly different results (both in strength and direction) when run with the same parameters. In at least 9 runs for each node, similar results were obtained.

## *T1R* and *LPH* cloning and functional testing

### Expression vector cloning and chimera design

*T1R*s from *Lepidothrix coronata* and *Neopelma chrysocephalum* were cloned from genomic DNA extracted using the DNeasy Blood & Tissue Kit (Qiagen); exons were determined using *T1R* predictions obtained from the genome assemblies. Deduced exons were amplified and assembled using a homology-based directional cloning method (In-Fusion cloning, Clontech) as previously described.[51,52,138] *LPH* predictions were curated from the manakin genomes, the chicken genome, the genome of an antbird, an umbrellabird, as well as from a draft assembly of a rusty-margined flycatcher; these predictions were synthesized (GENEWIZ). *T1R* and *LPH* expression vectors, as well as synthesized ancestral enzymes and receptors, ancestral *T1R* receptor chimeras, and point mutants of *LPH* were prepared using the pEAK10 vector (In-Fusion cloning, Clontech).

### Functional assays of T1Rs and LPH

Functional assays of T1Rs in HEK293T cells (a gift from the Matsunami laboratory, Duke University, USA) were performed using a luminescence assay, as recently described.[51,52,138] Functional assays of lactase-phlorizin followed the protocol developed for sucrase-isomaltase,[139] with minor modifications. For this assay, HEK293T (DSMZ-Leibniz Institute, #ACC 635) cells were transfected (700 ng plasmid), and incubated with 150 μL of either 66.67 mM lactose or 1.67 mM phlorizin dissolved in PBS for two hours; free glucose (as an indicator of enzymatic activity) was assessed with a glucose and sucrose assay kit (ab83387, Abcam). Following incubation, 50 μL of cell supernatant was added to 50 μL of assay master mix, and responses were compared to responses of control (mock-transfected) cells without addition of expression vectors.

## Structural model

The homology model of the heterodimer of the ancestral manakin T1R1-T1R3 was constructed as recently described.[52,138] The program Maestro (Schrödinger Suite 2019-1) was used, and the active form of mGluR5 (PDB ID: 6N51) served as a template.

# QUANTIFICATION AND STATISTICAL ANALYSIS

## RNA-seq quantification

The STAR quantified raw read counts of each gene were converted to RPK (Reads per Kilobase) by dividing raw read counts by the gene length (in kilobases). The gene lengths (the sum of non-overlapping exons) were extracted from the manakin annotation using the GenomicFeatures R package (version 1.48.4).[112] The RPK was normalized using the ''calcNormFactors'' function of the edgeR R

Please cite this article in press as: Balakrishnan et al., Genomic and physiological changes in a sexually selected and frugivorous bird radiation, Current Biology (2026), https://doi.org/10.1016/j.cub.2026.05.021





package (version 3.38.4)[113] and counts per million (CPM) calculated using the "cpm" function. For the top 20 highly expressed genes of the manakin transcriptomes (Figure S4E), we ranked the gene expression for each tissue type by geometric mean and plotted the expression values of the top 20 genes with the highest expression value per tissue (plotted from highest to lowest, per tissue).

We examined overlap between muscle-related genes under selection in *Manacus* and genes with evidence of expression changes in *M. vitellinus and Ceratopipra mentalis*.[12] Gene expression from the 'superfast' *scapulohumeralis caudalis* as well as the *pectoralis*, as a control, was compared using PhyDGET (Phylogenetic Differential Gene Expression Tool).[12] PhyDGET is a comparative approach to identify expression changes in a phylogenetic context and compares alternative models of evolution relative to a null expectation. We were particularly interested in genes that show either *Manacus* lineage specific changes (MV model) or shared changes in *Manacus* and *Ceratopipra* (MCC model in[12]). We used a BayesFactor threshold of 0.4 and conducted *post-hoc* pairwise Tukey tests in R (aov function, $p < 0.01$) between *M. vitellinus* and two species without rapid wing displays (*L. coronata* and *Pseudopipra pipra*) following the approach in.[33] Counts per million (CPM) were plotted as described in.[12]

### Permutation test for UCNE–gene clustering

To test whether specific genes were associated with more manakin-divergent UCNEs than expected by chance, we performed a permutation (randomization) test in R using the UCNE–gene association table (closest gene per UCNE as in Table S3). We generated an empirical null distribution by randomly sampling 99 UCNEs (the number of UCNEs in the manakin-divergent set) from the full UCNE set (n = 4,351) without replacement, recalculating UCNE counts per gene for each random draw, and repeating this procedure for 10,000 permutations. For each gene, the empirical one-tailed p-value was computed as the proportion of permutations in which the randomized count for that gene was greater than or equal to the observed count (adding a +1 pseudocount to numerator and denominator to avoid zero p-values). P-values were adjusted across all tested genes using the false discovery rate (FDR) procedure, and genes with FDR < 0.05 were considered significant.

### Composition of manakin-consumed fruits

We examined manakin fruit consumption data we collected for a recent paper on avian frugivory[54] in which we searched the databases Google Scholar, Scopus, and Web of Science using the terms "bird", "avian", "frugivory", "seed dispersal", and their Portuguese and Spanish equivalents for studies that reported the number of feeding visits by birds to focal fruiting plants. We used a subset of the dataset analyzed in[54] and focused on four passerine families (two suboscines, Pipridae and Tyrannidae, as well as two frugivorous oscine families, Thraupidae and Turdidae), including information from 47 studies conducted in a variety of regions, biomes and habitats, and data from 59 plants species.

### Lipid intake by bird family

From this dataset, we examined the number of visits of members of the four focal bird families. To assess the relative amounts of lipids consumed across the four families, we multiplied the number of visits by the average lipid content for that plant species, summed this for each of the four bird families, and divided by total visit numbers (mean and SEM represent % lipid content, weighted by visit numbers) (Figure S4) using the entries for these families. A total of 19508 visits to fruiting plants were considered, distributed as follows: Pipridae (1131), Thraupidae (8093) Turdidae (4689), Tyrannidae (5513). We also examined the number of visits to lipid-rich (defined as fruits with a lipid content on a dry mass basis $\geq$ 10%) and lipid-poor (fruits with < 10% lipids) fruits for each of the four families, and also tested if a negative correlation existed in this dataset between lipid content and percent of non-structural carbohydrates, as has been shown by other studies (Pearson correlation: $r = -0.51$, $n = 108$, $p < 0.001$).

### T1R/LPH functional statistics

For taste receptor experiments, statistical analyses of significant ligand-evoked luminescence responses were compared to responses from no-ligand controls (Figures 3 and S3E) or parent receptor constructs (Figure S3D), or, for dose-responses curves, between the receptors presented with the highest and lowest concentrations (Figure 3B) using Welch's one-tailed *t*-tests (multiple testing was controlled using the false discovery rate (FDR)); assays of enzymatic function compared fluorescence in transfected cells to that of untransfected cells after incubation with the same substrates (Figure 4) (Welch's one-tailed *t* tests; FDR correction for multiple testing).

### Comparative analyses of suboscine traits

#### *Dual precursor model of diet shifts*

Information on diet,[69] plumage scores for males and females,[68] and breeding system[67] were taken from published databases, and mapped on a recent phylogeny of suboscines[70]; amount of dietary fruit was visualized on the phylogeny (using the function 'contMap' in phytools[114]). To determine shifts in diet, we used a hidden Markov model to reconstruct the likely evolutionary history of frugivory in suboscines. Because low-level fruit consumption is widespread across many bird clades (both within and outside of suboscines), but fruit-dominated diets are much rarer and may require additional physiological adaptations, we implemented a model that incorporated two precursor states. For our initial model, we created three observed states: a diet lacking fruit, a low fruit diet (10-70% fruit in diet, following Wilman), and a high fruit diet (> 70%). Using corHMM (version 2.7),[115] we then created a 9 x 9 matrix to capture possible transitions between the three observed states and the three rates of a two-precursor model. We disallowed certain shifts within the model such that low and high fruit diets were not permitted states in the first rate class, a high fruit diet was not permitted

Please cite this article in press as: Balakrishnan et al., Genomic and physiological changes in a sexually selected and frugivorous bird radiation, Current Biology (2026), https://doi.org/10.1016/j.cub.2026.05.021



in the second rate class, and shifts to the third rate class required first evolving into the second rate class. Initially we set rate shifts within each class and between rate classes to be equal to one another, but we subsequently allowed rates both within a rate class and then between rate classes to vary. We also created a simpler single-precursor model, where the origin of the precursor allowed shifts to either low- or high-fruit diets, and experimented with allowing rates to vary between states with this set of models. After comparing AICc (corrected Akaike information criterion) scores across the fitted models, we found that a two-precursor model where we allowed rates to vary both within and between rate classes was the most well-supported model (lowest AICc score by > 2). We used this model to reconstruct the likely origin of both precursors, as well as the observed states of low and high fruit in the diets of suboscines, and summarized these results using the package shiftPlot.[116]

### Shifts in breeding, diet, and plumage traits

Next, we developed a method to link evolutionary shifts in the state of discrete traits to shifts in inferred evolutionary optima for continuous traits. The method shares many similarities with a recently-developed Bayesian approach incorporating trait ontologies[140] (which however does not yet handle covarying continuous characters, a key aspect of our analysis here). We were interested to test whether shifts in the presence or absence of biparental care were associated with shifts in the inferred clade-level optimum of a suite of three covarying characters: degree of frugivory, male plumage coloration, and female plumage coloration. We chose the latter two characters because strong sexual selection has been found to be associated not only with an increase in male plumage coloration, but more importantly with a simultaneous decrease in female plumage coloration.[68] Furthermore, it has been hypothesized that an increase in diet composition towards readily accessible, high-calorie food such as fruit can result in a loss of biparental care, via a number of possible mechanisms (availability of energy for complex displays, emancipation of males from parental care[3,20–22]); however, the association of diet and loss of parental care has not yet been formally examined.

For analysis of breeding system data, we converted the ordinal data of Tobias[67] into a binary dataset (Figure 5A), where 0 indicated a breeding system with biparental care, and 1 indicated a breeding system that lacked biparental care; as we were primarily interested in the complete loss of biparental care, the distinction between short-term and long-term bonds is less relevant here. A hidden state single precursor model was implemented in corHMM (version 2.7)[115] in which we allowed nodes to shift into the observed state of lacking biparental care only after first transitioning into a second rate class (representing a scenario in which this clade had evolved the necessary suite of traits to facilitate a loss of biparental care). Next, we used PhylogeneticEM[117,118] to fit a scalar Ornstein-Uhlenbeck model to identify rapid adaptive shifts in the inferred evolutionary optima of our correlated suite of continuous characters (male and female color, as well as fruit, here treated as a continuous variable). Shift points in the PhylogeneticEM analysis were identified and clades were collapsed (except in instances where subsequent downstream reversions occurred) and visualized using shiftPlot,[116] and colored according to the first axis of a principal component analysis of optima of fruit, male plumage, and female plumage. Shifts along branches leading to terminal taxa were disallowed. To examine the correspondence between these two sets of evolutionary shifts we extracted and compared the returned shift set from each of the discrete (here, examining shifts in the observed state of lacking biparental care, not the hidden precursor) and continuous models (the analysis of fruit and plumage) and explored the intersection of matched nodes (where shifts were determined in both analyses). This is a conservative approach in that both corHMM and PhylogeneticEM penalize the addition of shifts to the best fit model, and thus any shifts in state are already well-supported statistically.[115,117,118] As a further measure of conservatism, it is entirely possible that due to differences in how equivalent and well-supported shifts are interpreted by corHMM and PhylogeneticEM, our approach would miss shifts that if, interpreted slightly differently, would be concordant between the discrete and continuous datasets.

Next, we sought to derive a measure of significance for the concordance between these shifts by creating a null distribution of possible shift points in biparental care given the observed transition rate matrices. To do so, we first used the "makeSimmap" function of corHMM to simulate 1,000 stochastic character maps using the solution from the precursor model for breeding system described above. Second, we extracted the solution and converted it into the format required by the phytools function "sim.history". We treated each state, regardless of the rate class from corHMM, as its own state for the purposes of this function. To derive a root prior for "sim.history", we used the tip values and the "fitSYM" function of phytools to return a vector of estimated probabilities (a symmetrical transition matrix was favored for this stage over equal rates or all rates different). We passed this root prior to "sim.history" along with the modified solution matrix from corHMM to generate a separate set of 1,000 stochastic character maps. The critical difference between these and the maps generated with the "makeSimmap" function are that the latter were conditioned on the observed tip values, whereas the former incorporates only the inferred transition rate matrix, but no information on the observed tip values. In this way, we created a null distribution of 1,000 shift sets, which we could compare to the observed set of possible shifts conditioned on the tip values and the inferred hidden rates transition matrix.

We detect strong and well-supported concordance between shifts in frugivory and male and female coloration and losses of biparental care in suboscines. In total across the 1,000 stochastic character maps from corHMM we detected six concordant shifts in inferred state of biparental care and shifts in evolutionary optima of fruit + male color + female color (Figure S5D; Table S4). Some of these shifts were returned in nearly all of the 1,000 maps (in manakins, asities, and *Mionectes* flycatchers, Figure 5B), whereas others occurred infrequently. Comparing the observed concordant shifts with those from the null model, fewer nodes on average were found in common between the PhylogeneticEM results and simulated shifts in biparental care (Figure S5C, Wilcoxon rank sum test $p < 0.001$). We examined each of the six concordant shift points, and tallied how frequently shifts were observed in the null stochastic character maps on those same six nodes. Notably, the shifts which were less frequently returned in the stochastic

Please cite this article in press as: Balakrishnan et al., Genomic and physiological changes in a sexually selected and frugivorous bird radiation, Current Biology (2026), https://doi.org/10.1016/j.cub.2026.05.021





character maps conditioned on the observed tip data (i.e., Tyrannida, cotingas, and *Calyptoma*) were actually observed more often in the simulated data than in the observed data. In these three clades, shifts in plumage or fruit are associated with a reversion to biparental care, underscoring complex dynamics in these clades—in particular with cotingas—that will be interesting to explore in future studies. Thus, in summary, although some of these individual shifts are less well-supported than others, three of the six concordant shifts (*Mionectes* flycatchers, manakins, and *Philepitta* asities) were observed across nearly all runs, and appear to be particularly clear cases where increases in fruit and changes in plumage (in particular, decreases in female coloration) are associated with a loss of biparental care.